Oh, Tae Kyoo

CORRELATION OF THE TRANSIENT ENERGY MARGIN TO OUT-OF-STEP IMPEDANCE RELAY OPERATION

Iowa State University PH.D. 1986

PLEASE NOTE:

In all cases this material has been filmed in the best possible way from the available copy. Problems encountered with this document have been identified here with a check mark __✓__.

1. Glossy photographs or pages _____
2. Colored illustrations, paper or print _____
3. Photographs with dark background _____
4. Illustrations are poor copy _____
5. Pages with black marks, not original copy _____
6. Print shows through as there is text on both sides of page _____
7. Indistinct, broken or small print on several pages ✓
8. Print exceeds margin requirements _____
9. Tightly bound copy with print lost in spine _____
10. Computer printout pages with indistinct print _____
11. Page(s) _____ lacking when material received, and not available from school or author.
12. Page(s) _____ seem to be missing in numbering only as text follows.
13. Two pages numbered _____. Text follows.
14. Curling and wrinkled pages _____
15. Dissertation contains pages with print at a slant, filmed as received _____
16. Other _____

_____

_____

Correlation of the transient energy margin to Out-of-Step impedance relay operation

by

Tae Kyoo Oh

A Dissertation Submitted to the
Graduate Faculty in Partial Fulfillment of the
Requirements for the Degree of
DOCTOR OF PHILOSOPHY

Department: Electrical Engineering and Computer Engineering
Major: Electrical Engineering (Electric Power)

Approved:

Signature was redacted for privacy.
In Charge of Major Work

Signature was redacted for privacy.
For the Major Department

Signature was redacted for privacy.
For the Graduate College

Iowa State University
Ames, Iowa
1986

TABLE OF CONTENTS

LIST OF TABLES

LIST OF FIGURES

CHAPTER I. INTRODUCTION

Direct Transient Stability Analysis

Need for direct methods

The transient stability of a power system is the property of the system which insures that it reaches an acceptable steady-state operating condition following a large disturbance [1].

As power systems grow larger and more complex with the ever-increasing demand for electrical energy, they are required to be planned, designed, and operated to maintain a high degree of reliability. The stability of power systems is closely related to the question of whether the reliable and uninterrupted electric service can be maintained.

The issue of stability arises when a power system is disturbed. The stability problem is closely associated with the nature or magnitude of a disturbance. If the disturbance to which the power system is subjected is large, the oscillatory transient will also be large. The question then becomes, whether after these swings, the system will settle to a new acceptable operating state, or the large swings result in loss of synchronism. This is known as the transient stability problem.

Power systems are subjected to a large disturbance such as a sudden change in load, generation, or transmission system configuration due to faults or line switching. As a result, the transient stability analysis has become very important in all stages of power system

planning and operation in order to secure normal operation.

Conventionally, transient stability analysis of a power system is conducted by time simulation. In this method, a set of differential equations coupled with another set of algebraic equations, are solved numerically to obtain the power system dynamic behavior. The method is robust, reliable, and widely accepted by the utility industry. It is, however, computationally intensive and time-consuming. It does not provide a relative measure of the degree of stability or instability. Since time solution is conducted for one scenario at a time, limits can be derived only by repeated simulation.

At the present time as pointed out in the preface of reference [2] power systems in North America have become increasingly interconnected and tend to operate closer to their stability limits because of the unavailability of transmission corridors and increased loading of the transmission lines. The conventional technique has become inadequate in terms of providing quick answers to changing scenarios. There is a definite need for new analytical tools to tackle this problem. Direct methods of transient stability analysis have emerged as potential candidates to meet this requirement.

Progress and application

In the application of the direct methods to the analysis of power system stability, the well known equal area criterion [3,4] has been known for many years. This criterion provides good physical insight into the dynamic behavior of one machine-infinite bus system in terms of the conversion the kinetic energy into potential energy as the

generator torque angle swings during the transient. However, this criterion cannot be directly applied to a multimachine power system.

For the direct transient stability analysis of a multimachine power system, Gorev [in 5], Magnuson [6] and Aylett [7] developed energy-based methods using the first or energy integral of the swing equations which describe the power system dynamics following a disturbance. Following this initial work, Gless [8] and El-Abiad and Nagappan [9] applied Lyapunov's second method to power systems.

The basic idea behind these methods can be summarized as follows:

1. The swing equations describe the dynamics of the power system. These are a set of ordinary differential equations.
2. The transient stability analysis of the power systems deals with the system's capability of surviving the transient following a major disturbance, i.e., stability property of a post-disturbance network. The direct transient stability analysis is equivalent to the investigation of the stability properties of the post-disturbance equilibrium point. It is often referred to as a qualitative analysis of ordinary differential equations in mathematics [10].
3. A suitable scalar function, either the transient energy function or Lyapunov's function, is derived. For the purpose of estimating the region of stability the critical value of the functions is determined such that if the function's value at the end of disturbance is less than its critical value, the system is said to be stable for a

particular disturbance. The theoretical aspect of this development is treated in references [10-13].

From the viewpoint of practical application of these methods, numerous researchers have worked on two main issues: i) the development of suitable functions and ii) determination of their critical values. The survey papers by Fouad [13] and Ribbens-Pavella [14] and the book by Pai [12] have summarized the development on these issues.

In the course of development, energy-based methods seem to have been favored by many power engineers in North America because they provide better practical results.

Significant progress has been made in the direct transient stability analysis using energy-based methods. They are often referred to as Transient Energy Function (TEF) method in recent literature. The progress in the transient energy function method can be summarized as follows:

1. A center of inertia (COI) frame of reference is used in formulating the transient energy function. The importance of this formulation is in clearly focusing on the motion that tends to separate one or more machines from the rest of the system and in removing a substantial component of the system transient energy that does not contribute to instability, namely, the energy that either accelerates or decelerates the center of inertia [15-17]. With this formulation, the forces tending to separate some generators from the rest of the system and the energy components

associated with their motion can be easily identified [15,18,19]. Also this formulation provides a convenient way of incorporating the transfer conductance terms into the transient energy function.

2. The concept of a controlling unstable equilibrium point (u.e.p.) is validated [15,20]. The physical meaning of the controlling u.e.p. can be interpreted such that if a disturbance is critically cleared, the trajectory of post-disturbance system will pass through or nearby the u.e.p. The proper identification of this u.e.p. of interest is crucial because the critical energy is given by the potential energy evaluated at the u.e.p. with respect to the stable equilibrium point of the post-disturbance network. Hence, inaccurate determination of the u.e.p. results in erroneous stability assessment. The failure to determine a correct u.e.p. of interest has been a major source of conservative results. El-Abiad and Nagappan [9] determined the critical energy at the u.e.p. closest to the stable equilibrium point of the post-disturbance network. This implies that a generator which has the weakest coupling may lose synchronism with the system regardless of the nature and location of the disturbance. This could be the case in a small system but not in practical systems. Prabhakara and El-Abiad [21], Gupta and El-Abiad [22] and Athay et al. [18,19] took the fault location into account to determine a

relevant u.e.p. It was shown that the relevant u.e.p. to be considered is the one in the direction of the faulted trajectory and the generators whose rotor angles are greater than 90 degrees in the u.e.p. are actually losing synchronism when instability is initially encountered. This was an important breakthrough to overcome the difficulty of severe conservative results. However, it needed further improvement to explain the complex mode of disturbance that not all the severely disturbed machines lose synchronism initially. The mode of disturbance depends upon not only the fault location but also the energy absorbing capacity of the post-disturbance network. Therefore, the determination of the controlling u.e.p. must properly account for two aspects of the transient phenomena: i) the effect of the disturbance on the various generators, and ii) information on the energy absorbing capacity of the post-disturbance network [23]. From the investigation on the energy responsible for the separation of one or more generators from the rest of the system using individual energy function [24], Fouad et al. [23] developed a technique of determining the controlling u.e.p. by identifying the weakest link in the path of trajectory. In the controlling u.e.p. thus determined, a group of critical machines, i.e., severely disturbed machines are identified by angles generally greater than 90 degrees. These generators are severely

affected by the disturbance but are not necessarily the ones which lose synchronism initially.

3. The component of the transient energy that does not contribute to system separation was identified. It was shown in [15,20] that not all the kinetic energy at the instant of clearing the disturbance contributes directly to the separation of the critical machines from the rest of the system. Some of that energy accounts for the other intermachine oscillations. By correcting that component of kinetic energy from the energy that needs to be absorbed by the system for stability to be maintained, the stability assessment was substantially improved in terms of the computation of the critical clearing time in rather complex situations [15].

Application

In a recent paper [25], the status of the application of direct methods to transient stability analysis of power systems were reviewed. The use of the transient energy function method in such applications has been addressed in [26]. In fact, the transient energy function method has been successfully applied to practical power system problems in certain areas of North America. Among those applications are the following:

1. The method was applied to assess the transient stability of a power system at the end of a complex disturbance sequence which involves braking resistor switching, generation-

shedding, and high speed reclosing of the circuit breaker [27]. Following this assessment, the amount of generation-shedding required was estimated early in the disturbance sequence to prevent loss of synchronism.

2. The method was applied to determine the critical interface flows for various system outages and operating conditions using the unnormalized energy margin sensitivity [28].
3. The method was applied to the analysis of loss of generation disturbance [29].
4. The method was applied to analyze a conventional transient stability program output, using individual machine energy functions. A qualitative index of the degree of stability or instability for each generator was provided for a given stability run. This index is useful for guiding the selection of subsequent case studies [30].
5. The method was applied to the transient stability analysis of large and realistic power systems [31].

Current research is under way to extend the application of the transient energy function method to larger systems [31] and disturbances other than faults [30] and continues to expand the areas of application of the technique.

Statement of the Problem

Motivation for the research

The applications of the transient energy function method to the direct transient stability analysis of a power system have been briefly reviewed in the previous section. Among the applications which received some attention in the literature is the use of the TEF method to detect instability and/or out-of-step operation and initiate the out-of-step relay operation. This issue will be of particular interest in the event that system separation takes place not because of instability following a particular disturbance but because of the protective relay, more specifically, out-of-step impedance relay operation. This is true because out-of-step relays are often set to operate below the point where loss of synchronism actually occurs so that a severe swing of the voltage and power can be prevented.

Conceptually, for the analysis of out-of-step(OS) relay operation, the portion of a system on either side of tie line(s) protected by OS relay(s) is represented by an equivalent machine and the equal area criterion is applied to the equivalent [32-34]. Based upon this concept, a procedure was developed in [29,35], which relates the transient energy margin obtained from a multimachine system to minimum apparent impedance seen by the out-of-step relay in the two machine equivalent formulated using EPRI's coherency-based dynamic equivalencing program [36]. Although the analysis in the two machine equivalent is somewhat straightforward, the cost of obtaining such an equivalent from large systems may diminish its merit.

In this research work, a technique for monitoring out-of-step impedance relay operation will be developed by correlating the energy margin to the minimum apparent impedance seen by OS relay in a multimachine power system.

Scope of the Work

The objectives of this research work are

1. Development of a criterion for determining the maximum swing angles along the trajectory of the post-disturbance system. This is the point where the apparent impedance seen by out-of-step impedance relay at the electrical center of the system becomes minimum.
2. Development of a technique for approximating the trajectory of the post-disturbance system so that the maximum swing angles can be determined without solving the system differential equations by numerical step-by-step integration method.
3. Development of a procedure for obtaining the swing impedance locus utilizing the above two steps in a multimachine power system reduced to the internal nodes of generators with relay buses retained.

CHAPTER II. TRANSIENT ENERGY FUNCTION METHOD FORMULATION

Power System Representation and Transient Energy Function

For transient stability analysis by the transient energy function(TEF) method, the power system is represented by the so-called classical model [12-24]. This model is based on the following assumptions [37]:

1. The transmission network is modeled by steady-state equations.
2. Mechanical power input is constant.
3. Damping or asynchronous power is negligible.
4. The synchronous machine is represented by constant voltage source behind its transient reactance.
5. The motion of the rotor of a machine coincides with the angle of the voltage behind the transient reactance.
6. Loads are represented by constant passive impedances.

Based on these assumptions, the swing equations that govern the dynamics of the system are given by

$$M_i\dot{\omega}_i = P_i - P_{ei}$$
$$\dot{\delta}_i = \omega_i \quad \text{for } i=1,2,\ldots n \tag{2.1}$$

where

$$P_{ei} = \sum_{\substack{j=1 \\ j\neq i}}^{n} [C_{ij}\sin(\delta_{ij}) + D_{ij}\cos(\delta_{ij})]$$

$$P_i = P_{m_i} - E_i^2 G_{ii}$$

$$C_{ij} = E_i B_{ij} E_j, \quad D_{ij} = E_i G_{ij} E_i$$

P_{mi} - mechanical power input

E_i - constant voltage behind its transient reactance

G_{ii} - driving point conductance

M_i - inertia constant

ω_i, δ_i - generator rotor speed and angle deviation, respectively, with respect to a synchronously rotating reference frame.

$G_{ij}+jB_{ij}$ - the transfer admittance in the system reduced to the internal node of generators i and j, respectively.

The system equation (2.1) are written with respect to an arbitrary synchronously rotating frame of reference. One of key steps in the TEF formulation is to transform these equations into the center of inertia (COI) coordinate. This formulation clearly focuses on the mechanism of separation of one or more generators from the rest of the system and removes the component of the transient system energy that does not contribute to the instability.

In order to transform the system equations (2.1) into the center of inertia coordinate, define

$$M_T \triangleq \sum_{i=1}^{n} M_i$$

$$\delta_o \triangleq \sum_{i=1}^{n} M_i\delta_i/M_T$$

Then

$$M_T\dot{\omega}_o \triangleq \sum_{i=1}^{n} M_i\dot{\omega}_i = \sum_{i=1}^{n} (P_i - P_{ei}) \triangleq P_{COI}$$

$$\dot{\delta}_o = \omega_o$$

We obtain new angles with respect to the center of inertia by defining

$$\theta_i \triangleq \delta_i - \delta_o$$

With this coordinate system the system equations become

$$M_i\dot{\tilde{\omega}}_i = P_i - P_{ei} - M_i/M_T\, P_{COI}$$

$$\dot{\theta}_i = \tilde{\omega}_i \qquad \text{for } i=1,2,\ldots,n \tag{2.2}$$

By definition, we have the constraints:

$$\sum_{i=1}^{n} M_i\theta_i = 0, \text{ and}$$

$$\sum_{i=1}^{n} M_i\tilde{\omega}_i = 0 \tag{2.3}.$$

The equilibrium points of the system are the points which satisfies

$$0 = P_i + P_{ei} - M_i/M_T\, P_{COI}$$

$$0 = \tilde{\omega}_i$$

Among such equilibrium points, the stable equilibrium point(s.e.p.), $\underline{\theta}^s$ and the controlling unstable equilibrium point(u.e.p.), $\underline{\theta}^u$ are of interest for the purpose of direct transient stability analysis by the TEF method.

From the system equations(2.2) and the first integral, we can show that the transient energy function, V is given by

$$V = 1/2\sum_{i=1}^{n} M_i\tilde{\omega}_i^2 - \sum_{i=1}^{n} P_i(\theta_i - \theta_i^s)$$

$$- \sum_{i=1}^{n-1} \sum_{j=i+1}^{n} [C_{ij}(\cos(\theta_{ij}) - \cos(\theta_{ij}^s)$$

$$+ \int_{\theta_i^s + \theta_j^s}^{\theta_i + \theta_j} D_{ij}\cos(\theta_{ij})d(\theta_i + \theta_j)] \qquad (2.4)$$

where $\underline{\theta}^s$ is the stable equilibrium point of the post-disturbance system. The transient energy in equation (2.4) is composed of two components: i) the kinetic energy which is represented by the first term, and ii) the potential energy which is represented by the rest of terms. The fourth term which represents the energy dissipated in the network transfer conductances is a path-dependent integral. This term can be calculated only if the system trajectory is known. For the purpose of the analysis by the direct method, this term can be approximated with the linear approximation of trajectory as follows [20, 38]:

$$I_{ij} = D_{ij}((\theta_i + \theta_j - \theta_i^s - \theta_j^s)/(\theta_{ij} - \theta_{ij}^s))(\sin\theta_{ij} - \sin\theta_{ij}^s) \qquad (2.5).$$

The Critical Energy and the Transient Energy Margin

The critical energy is the potential energy evaluated at the controlling u.e.p. with respect to the stable equilibrium point of the post-disturbance system [15,20]. Hence, the identification and computation of the controlling u.e.p. is a key step of the transient energy function method [15,23]. The transient energy margin is defined as the difference between the critical energy and the transient energy

that the system possesses at the end of disturbance [15,20]. For the purpose of the numerical computation, the transient energy margin, ΔV is given by

$$\Delta V = V\Big|_{\theta^s}^{\theta^u} - V\Big|_{\theta^s}^{(\theta^{cl},\ \tilde{\omega}^{cl})} = V\Big|_{(\theta^{cl},\ \tilde{\omega}^{cl})}^{\theta^u}$$

$$= -1/2\sum_{i=1}^{n} M_i\tilde{\omega}_i^{cl2} - \sum_{i=1}^{n} P_i(\theta_i^u - \theta_i^{cl})$$

$$- \sum_{i=1}^{n-1}\sum_{j=i+1}^{n} [C_{ij}(\cos\theta_{ij}^u - \cos\theta_{ij}^{cl}) - I_{ij}] \qquad (2.6)$$

where

$$I_{ij} = D_{ij}((\theta_i^u+\theta_j^u-\theta_i^{cl}-\theta_j^{cl})/(\theta_{ij}^u-\theta_{ij}^{cl}))(\sin\theta_{ij}^u - \sin\theta_{ij}^{cl})$$

If the transient energy margin, ΔV is positive at the instant of clearing disturbance, the system is stable. Otherwise the system is unstable.

The Kinetic Energy Correction

A large disturbance tends to split the system into two groups of machines which are a group of critical machines and a group consisting of the rest of the system. In the controlling u.e.p., the group of critical machines i.e., severely disturbed machines are identified by angles greater than 90 degrees. The kinetic energy which is responsible for the separation of the critical machines from the rest of the system is that associated with the gross motion of two groups of

machines. The remaining portion of the kinetic energy accounts for the other intermachine swings. For stability analysis, that component of kinetic energy should be subtracted from the energy that needs to be absorbed by the system for stability to be maintained. This is done by the kinetic energy correction as follows [15,20]:

$$V_{KE|corr} = 1/2 M_{eq} \omega_{eq}^2$$

where

$$M_{eq} = (M_{cr} \cdot M_{sys})/(M_{cr} + M_{sys})$$

$$\omega_{eq} = \omega_{cr} - \omega_{sys}$$

M_{cr} - the sum of inertia constant of critical machines

M_{sys}- the sum of inertia constant of the rest of the system

ω_{cr} - the angular speed at the inertial center of critical machines

ω_{sys}- the angular speed at the inertial center of the rest of the system

This is the corrected kinetic energy that is to be used to compute the transient energy margin.

Stability Assessment by the TEF Method

The system transient energy V is evaluated with respect to the post-disturbance equilibrium conditions. Its critical value V^u is given by the value of the potential energy at the controlling u.e.p. for the particular disturbance under investigation. Transient stability assessment is made by computing the difference between the

the value of V at the end of the disturbance and V^u. Stability is maintained if $V^u > V$, or if the energy margin $\Delta V = (V^u - V) > 0$. Otherwise the system is unstable.

CHAPTER III. THE MINIMUM APPARENT IMPEDANCE SEEN BY THE OUT-OF-STEP RELAY PREDICTED BY THE TRANSIENT ENERGY MARGIN

Introduction

One of the objectives of transient stability analysis of power systems is to analyze the setting and operation of protective relays. In certain situations when a power system is disturbed, a group of severely disturbed, i.e., critical machines, tends to separate from the rest of the system. When the two groups of generators tend to lose synchronism with each other, the continuing fluctuations of voltage and power in the system severely disrupt service. This is known in the industry as out of step operation, and is detected by special "out-of-step" relays. It is advisable to separate the two groups of machines by initiating out-of-step relay action so that the cascading effects of such objectionable swings can be prevented. In certain other cases a single machine running out of step with other machines on the same bus may not only impair service but may also suffer damage itself. Hence, such a machine should be disconnected as soon as possible just before it falls out-of-step [32].

From the interconnected system performance point of view, the out-of-step relaying scheme should initiate tripping before the voltage at the electrical center swings to a minimum value. This prevents severe voltage dips and power fluctuations throughout the power system without uncontrolled loss of loads. Another aspect of out-of-step relay schemes, setting, deals with the ability to distinguish between faults

and swings. Tripping on recoverable swings should be avoided [39, 40].

Since relaying schemes must function properly during system swings, it is necessary to understand the effects of these swings on relay performance. The portion of the system on either side of the tie lines protected by out-of-step relays can be represented as an equivalent generator. Such an equivalent can be obtained with reasonable accuracy by incorporating the effects of the disturbance and using appropriate techniques such as coherency-based dynamic equivalencing. This approach has been generally adopted for the analytical study of out-of-step relay schemes [32-34]. The effects of the swings and the operation of out-of-step relays can be analyzed using the two machine equivalent because the equivalent accounts for the gross motion of the two groups of generators.

Recently, direct methods have been used to detect instability and/or out-of-step operation and initiate the appropriate relay action. Roemish and Wall [41] applied Lyapunov's direct method to determine the stability boundary for a two-machine system, one machine being the protected generator, or the plant, and the other machine being the interconnected system regarded as a single equivalent machine. They used two ways of modeling the system in the formulation of the method, one being the classical model and the other being more detailed model with some control devices. If out-of-step operation is detected, tripping of relaying system is initiated to protect the generator or the plant. Ohura et al. [42] applied the transient energy function method to the development of a generator tripping relaying system to

enhance transient stability of the system. Fouad et al. [29] and Vittal, Oh, and Fouad [35] developed a procedure of correlating the transient energy margin to minimum apparent impedance seen by the out-of-step relay. The approach developed in references [29,35] is of particular interest because it studied the issue of system separation due to out-of-step relay operation before loss of synchronism is encountered. This aspect is of significance in developing security assessment schemes, where it is essential to determine in advance the response of a system to a particular disturbance.

The Minimum Apparent Impedance Seen by the Out-of-Step Relay and the Maximum Swing Angles

The apparent impedance seen by the out-of-step relay changes as the two groups of machines on either side of the line protected by the relay swing with respect to each other. In general, the out-of-step relay is set with the assumption that the apparent impedance seen by the relay located at or near the electrical center becomes minimum in terms of distance from the center of the relay zone when the angular swings reach their maximum. In a two machine system, the minimum apparent swing impedance is then determined using the equal area criterion which provides the information about the maximum angular swing.

Based on this concept, a relation was developed between the transient energy margin and the minimum apparent swing impedance by relating the normalized transient energy margin of the multimachine

system to the ratios of the areas used in the equal area criterion [29,35]. However, this requires the intermediate step of constructing a coherency-based two machine equivalent. In this research work, the intermediate step will be eliminated. The transient energy margin will be directly related to the maximum swing angles, in turn, related to the minimum swing impedance, using multimachine parameters.

Energy Constraints on the System Dynamics of the Post-disturbance Network

Total system energy

When a power system is disturbed, energy is injected into the system and the excess energy which the system possesses at the end of disturbance is the transient system energy. This energy is associated with system dynamics of the post-disturbance network. Since there is no energy injected into the system after the disturbance is removed, the transient system energy is constant in the post-disturbance period. Therefore, the energy integral along the trajectory of post-disturbance system with respect to the point where the disturbance is removed should be equal to zero. If one states this condition mathematically, it will become

$$V\Big|_{(\underline{\theta}^{cl},\ \underline{\tilde{\omega}}^{cl})}^{(\underline{\theta},\ \underline{\tilde{\omega}})} = 0 \qquad (3.1)$$

where

$(\underline{\theta}^{cl},\ \underline{\tilde{\omega}}^{cl})$: angular position and

velocity vector respectively at the instant of disturbance removal.

$(\underline{\theta}, \underline{\tilde{\omega}})$: angular position and velocity vector respectively along the trajectory of the post-disturbance network.

or

$$1/2 \sum_{i=1}^{n} M_i \tilde{\omega}_i^2 - 1/2 \sum_{i=1}^{n} M_i \tilde{\omega}_i^{cl2}$$

$$= \int_{\theta^{cl}}^{\theta} \sum_{i=1}^{n} (P_i - P_{ei} - M_i/M_T \, P_{COI}) d\theta_i \qquad (3.2)$$

or $$\Delta V_{KE} = - \Delta V_{PE} \qquad (3.3)$$

This shows that as in the one machine-infinite bus system the system dynamics in a multimachine system can be regarded as a phenomenon of energy conversion process from the kinetic energy to the potential energy or vice versa.

Two machine equivalent energy

As mentioned in the previous chapter, one of the important steps in the progress of the transient energy function method was the identification of the component of the transient kinetic energy that does not contribute directly to system separation [14, 18]. If more than one machine tends to lose synchronism with the system, instability is determined by the gross motion of these machines, i.e., by the motion of their inertial center with respect to the inertial center of

the rest of the system. In addition, the advanced machines in the controlling u.e.p. indicate the groups of those machines which swing away from the rest of the system. Using this information, one can formulate a two-machine equivalent which represents the gross motion of a multimachine system. One equivalent machine will represent the motion of the inertial center of the advanced group of machines and the other equivalent will represent that of the rest of the system. In doing so, parameters will be deduced only from the multimachine system and no physical equivalencing will be done. An energy function defined for the equivalents will focus on the dynamics of the two equivalents located at the fictitious inertial centers.

Without loss of generality, one can assume that the first K machines are the critical machines. The equations which represents the dynamics of the inertial centers of the two groups of machines can be obtained in the following manner. Referring to Equation (2.2), define

$$M_K \triangleq \sum_{i=1}^{k} M_i$$

$$M_{T-K} \triangleq \sum_{i=k+1}^{n} M_i$$

then

$$M_K\dot{\tilde{\omega}}_K \triangleq \sum_{i=1}^{k} M_i\dot{\tilde{\omega}}_i = \sum_{i=1}^{k} (P_i - P_{ei} - M_i/M_T\, P_{COI})$$

$$\triangleq P_K - P_{eK} - M_K/M_T\, P_{COI}$$

$$\dot{\theta}_K = \tilde{\omega}_K$$

$$M_{T-K}\dot{\tilde{\omega}}_{T-K} \triangleq \sum_{i=k+1}^{n} M_i\tilde{\omega}_i \triangleq \sum_{i=k+1}^{n} (P_i - P_{ei} - M_i/M_T\, P_{COI}$$

$$\triangleq P_{T-K} - P_{eT-K} - M_{T-K}/M_T\, P_{COI}$$

$$\dot{\theta}_{T-K} = \tilde{\omega}_{T-K} \tag{3.4}$$

where

$$P_K = \sum_{i=1}^{k} P_i$$

$$P_{eK} = \sum_{i=1}^{k} P_i$$

$$P_{T-K} = \sum_{i=K+1}^{n} P_i$$

$$P_{eT-K} = \sum_{i=k+1}^{n} P_{ei}$$

$$\theta_K = 1/M_K \sum_{i=1}^{k} M_i\theta_i$$

$$\theta_{T-K} = 1/M_{T-K} \sum_{i=k+1}^{n} M_i\theta_i$$

The equations (3.4) clearly focus on the motion of the inertial centers and eliminate some components of the force that is associated with the intermachine oscillation among the machines which belong to the same group.

Using the energy integral as in a multimachine system [20], V_i for the two machine equivalent is given by

$$V_{eq} = \int_o^t \{[M_K\dot{\tilde{\omega}}_K - P_K + P_{eK} + M_T P_{COI}]\dot{\theta}_K$$

$$+ [M_{T-K}\dot{\tilde{\omega}}_{T-K} - P_{T-K} + P_{eT-K} + M_{T-K}/M_T P_{COI}]\dot{\theta}_{T-K}\}dt$$

or

$$V_{eq} = 1/2\ M_K\tilde{\omega}_K^2 + 1/2\ M_{T-K}\tilde{\omega}_{T-K}^2 - P_K(\theta_K - \theta_K^s) - P_{T-K}(\theta_{T-K} - \theta_{T-K}^s)$$

$$+ \int_{\theta_K^s}^{\theta_K} P_{eK}d\theta_K + \int_{\theta_{T-K}^s}^{\theta_{T-K}} P_{eT-K}d\theta_{T-K} \qquad (3.5)$$

The first two terms represent the kinetic energy of the inertial centers of the two groups of machines. The next two terms represent the position energy of the inertial centers of the two groups of machines. The last two terms represent the components of energy which are associated with the electrical property of the system. They are the energy magnetically stored in the network and the energy dissipated over the conductance in the network.

There are two interesting points to note in the energy function, V_i as follows:

1. The kinetic energy of this energy function is equal to the corrected kinetic energy of the energy function of the multimachine system. Also, the position energy is equal to the equivalent position energy developed in [23].

2. The magnetic energy stored in the coupling between the machines within the same groups disappear. However, the energy dissipated over the conductance in the network is not affected by the equivalencing process.

Equations (3.5) contains terms that have path-dependent integrals. Evaluation of these integrals requires knowledge of the system trajectory.

Maximum Swing Angles Obtained by Energy Constraints

In a one-machine-infinite bus system the generator rotor acquires kinetic energy under the influence of the disturbance. After the disturbance is removed, the rotor will swing away up to the point where the kinetic energy is completely converted into the potential energy. This point is the maximum swing angle where equal area criterion is satisfied and the energy margin is defined. In Figure 1 area A_1 indicates the kinetic energy acquired during fault-on period. As the generator rotor swings along the torque angle curve of the post-disturbance network, the kinetic energy is converted into the potential energy indicated by area A_2. The value of the maximum angular swing δ^m corresponds to the condition that the area A_1 is equal to the area A_2. Area A_3 then provides the energy margin.

The same reasoning is applied to a multimachine system. The transient system energy will cause the generators' rotors to swing away to the point where the kinetic energy becomes minimum. For a stable system, it represents the condition where the critical machines (more

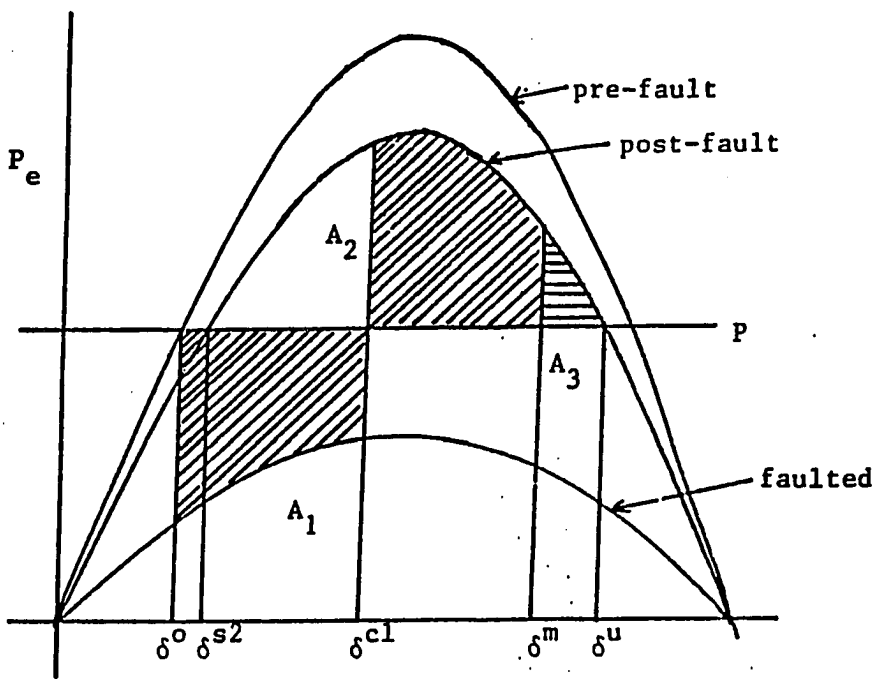

δ^o : initial operating point

δ^{s2}: post-fault equilibrium point

δ^{cl}: clearing angle

δ^m : maximum swing angle

δ^u : unstable equilibrium angle

FIGURE 1. The equal area criterion

specifically, their inertial center) are the farthest away from the rest of system. At that point while the system transient kinetic energy may not be zero, the corrected kinetic energy is exactly zero.

Considering the relative motion of the critical machines with respect to the rest of the system, the point in angular space at which the former group is at the their maximum swing is exactly when their inertial center is stationary with respect to the inertial center of the latter group. Thus, this point which we will designate (in the n-dimensional angular space) as $\underline{\theta}^m$ is the instant at which ΔV is made up exactly of potential energy. Since in the post-disturbance period the total transient energy is constant, the condition can be described as follows:

1. Using total system energy

$$\Delta V^{cl} \equiv \Delta V_{PE}^m$$

where

ΔV^{cl} - the system transient energy margin given by equation (2.6) at the instant of disturbance removal

$$\Delta V_{PE}^m = -\sum_{i=1}^{n} P_i(\theta_i^u - \theta_i^m)$$

$$-\sum_{i=1}^{n-1}\sum_{j=k+1}^{n} [C_{ij}(\cos\theta_{ij}^u - \cos\theta_{ij}^m)$$

$$-\int_{\theta_i^m + \theta_j^m}^{\theta_i^u + \theta_j^u} D_{ij}\cos\theta_{ij}\, d(\theta_i + \theta_j)] \qquad (3.6)$$

- the potential energy margin at the maximum swing angles $\underline{\theta}^m$

2. Using the fictitious two machine inertial-center equivalent energy

$$\Delta V_{eq}^{cl} \equiv \Delta V_{PEeq}^{m}$$

where

$$\Delta V_{eq}^{cl} = -1/2\ M_K \tilde{\omega}_K^{cl\,2} - 1/2\ M_{T-K}\tilde{\omega}_{T-K}^{cl\,2} - P_K(\theta_K^u - \theta_{T-K}^{cl}) + \int_{\theta_K^{cl}}^{\theta_K^u} P_{eK}\, d\theta_K + \int_{\theta_{T-K}^{cl}}^{\theta_{T-K}^u} P_{eT-K}\, d\theta_{T-K}$$

- the equivalent transient energy margin at the instant of disturbance removal

$$\Delta V_{PEeq}^{m} = -P_K(\theta_K^u - \theta_K^m) - P_{T-K}(\theta_{T-K}^u - \theta_{T-K}^m) + \int_{\theta_K^m}^{\theta_K^u} P_{eK}\, d\theta_K + \int_{\theta_{T-K}^m}^{\theta_{T-K}^u} P_{eT-K}\, d\theta_{T-K}$$

- the equivalent potential energy margin at the maximum swing angle, $\underline{\theta}^m$

CHAPTER IV. APPROXIMATION OF THE SYSTEM TRAJECTORY DURING THE FIRST SWING TRANSIENT

Introduction

In the previous chapter, two types of energy criteria have been derived to determine the maximum swing angles along the system trajectory of the post-disturbance network. The criteria use only the multimachine parameters. These criteria provide the vector of multimachine rotor angles $\underline{\theta}^m$ at which the two groups of machines on either side of the line protected by the out-of-step relay are separated farthest from each other. At this point the swing impedance seen by the out-of-step relay becomes a minimum. Hence, the operation of the out-of-step relay can be analyzed qualitatively as well as quantitatively when the maximum swing angles are known. However, in order to apply the criteria developed to compute the maximum swing angles, one needs knowledge of the the post-disturbance system trajectory. The true system trajectory can be obtained only by time simulation with appropriate modeling of a power system, which the direct method is trying to avoid in the first place. Hence, an approximation to the post-disturbance trajectory has to be determined. The two energy-based criteria developed in Chapter III are then applied along the approximation to the post-disturbance trajectory.

Two Point Boundary Value Formulation

As a guide to the approximation, we have information at two different points on the post-disturbance trajectory: i) at the removal of

disturbance, and ii) at the controlling u.e.p. Although the computation of the two points are not trivial, they are necessary for the stability assessment by the transient energy function method.

As we have seen in the previous chapters, the concept of the controlling u.e.p. is far-reaching. The physical significance of the controlling u.e.p. is that if a disturbance is cleared critically, the trajectory of the post-disturbance network will approach and pass at or nearby that point. Since transient stability analysis deals with a large disturbance, one can assume that the post-disturbance trajectory during the first swing transient moves in the direction toward the controlling u.e.p. from the point where the disturbance is removed. Using this information, one can formulate a two point boundary value problem to approximate the trajectory as follows:

- Let $f_i(\underline{\theta})$ denote the right hand side of the swing equation in (2.2). Since $f_i(\underline{\theta})$ is continuously differentiable with respect to time infinitely, the higher order derivatives of $\theta_i(t)$ exist and are continuous.

  The first and second derivatives of $f_i(\underline{\theta})$ are given by

$$\dot{f}_i(\underline{\theta}) = \nabla f_i(\underline{\theta})^T \cdot \tilde{\omega}$$

$$\ddot{f}_i(\underline{\theta}) = \tilde{\omega}^T \cdot \nabla^2 f_i \cdot \tilde{\omega} + \nabla f_i(\underline{\theta})^T \cdot \dot{\tilde{\omega}}$$

- Assume that at some finite point of time T, the critical trajectory is close to the controlling u.e.p.
- Let t=0 be the instant of disturbance removal.

  Then

$$\theta_i(0) = \theta_i^{cl}$$

$$\dot{\theta}_i(0) = \tilde{\omega}_i(0) = \tilde{\omega}_i^{cl}$$

$$\ddot{\theta}_i(0) = \dot{\tilde{\omega}}_i(0) = f_i(\theta^{cl})/m_i$$

$$\vdots$$

$$\theta_i^{(r)}(0) = \tilde{\omega}_i^{(r-1)}(0) = f_i(\theta^{cl})^{(r-2)}/M_i$$

where r indicates r^{th} derivative.

- At t=T

$$\theta_i(T) = \theta_i^{u}$$

$$\dot{\theta}_i(T) = \tilde{\omega}_i(T) = 0.0$$

$$\ddot{\theta}_i(T) = \dot{\tilde{\omega}}_i(T) = f_i(\theta^{u})/m_i = 0.0$$

$$\vdots$$

$$\theta_i^{(r)}(T) = \tilde{\omega}_i^{(r-1)}(T) = f_i(\theta^{u})^{(r-2)} = 0.0$$

where r indicates r^{th} derivative.

Approximation by Interpolation

The formulation in the previous section can be referred to as interpolation between two points with higher derivatives. From the information available, an approximation to the post-disturbance trajectory between the two points needs to be determined. There are several approaches to handle this problem [43]. From the practical application point of view, the linear interpolation and the Fourier series

interpolation are of interest [43, 44, 45].

The linear interpolation

This provides the simplest approximation of the trajectory. This approximation utilizes only the rotor angles at the two points as follows:

$$\theta_i(t) = \theta_i(0) + t(\theta_i^u - \theta_i(0))$$

$$0 \le t \le 1, \quad \text{for } i=1, 2, \ldots n \tag{4.4}$$

where time is normalized by T.

We have seen that the path-dependent integral for a multimachine system is usually evaluated with this approximation as in equation (2.5).

With this approximation, V_{eq} for the two machine equivalent is given by

$$V_{eq} = 1/2\, M_K \tilde{\omega}_K^2 + 1/2\, M_{T-K} \tilde{\omega}_{T-k}^2 - P_K(\theta_K - \theta_K^s) - P_{T-K}(\theta_{T-K} - \theta_{T-K}^s)$$

$$- \sum_{i=1}^{k} \sum_{j=k+1}^{n} C_{ij} \frac{(\theta_K - \theta_K^s) - (\theta_{T-K} - \theta_{T-K}^s)}{\theta_{ij} - \theta_{ij}^s} (\cos\theta_{ij} - \cos\theta_{ij}^s)$$

$$- \sum_{i=1}^{k} \sum_{j=k+1}^{n} C_{ij} \frac{(\theta_K - \theta_K^s) + (\theta_{T-K} - \theta_{T-K}^s)}{\theta_{ij} - \theta_{ij}^s} (\cos\theta_{ij} - \cos\theta_{ij}^s)$$

$$+ 2 \sum_{i=1}^{k-1} \sum_{j=k+1}^{n} D_{ij} \frac{\theta_K - \theta_K^s}{\theta_{ij} - \theta_{ij}^s} (\sin\theta_{ij} - \theta_{ij}^s)$$

$$+ 2 \sum_{i=1}^{k-1} \sum_{j=k+1}^{n} D_{ij} \frac{\theta_{T-K} - \theta_{T-K}^s}{\theta_{ij} - \theta_{ij}^s} (\sin\theta_{ij} - \theta_{ij}^s) \tag{4.5}$$

The Fourier series interpolation

Any periodic function can be represented by the Fourier series [44-46]. In the problem formulated in the previous section, the system trajectory over only the period [0, 1] is of interest with time being normalized by T.

In order to make use of the theory of the Fourier series, we can assume without loss of generality that the system trajectory is periodic with a period T. Then the system trajectory can be represented by the Fourier series as follows:

$$\theta_i(t) = a_{i0} + \sum_{k=1}^{\infty} (a_{ik}\cos(2k\pi t) + b_{ik}\sin(2k\pi t))$$

$$\text{for } i=1, 2, \ldots\ldots, n \qquad (4.6)$$

Then, the first and second derivatives of $\theta_i(t)$ will be

$$\dot{\theta}_i(t) = \sum_{k=1}^{\infty} ((-2k\pi)a_{ik}\sin(2k\pi t) + (sk\pi)b_{ik}\cos(2k\pi t))$$

$$\theta_i(t) = -\sum_{k=1}^{\infty} ((2k\pi)^2 a_{ik}\cos(2k\pi t) + (2k\pi)^2 b_{ik}\sin(2k\pi t)) \qquad (4.7)$$

From the practical application point of view, the above series can be truncated after some terms. There is another important factor to be considered. The computation of derivatives of $f_i(\underline{\theta})$ beyond the second order becomes so burdensome that the use of those terms may not be practical.

The determination of the coefficients of this series approximation depends on the initial condition of the post-disturbance network and the controlling u.e.p. The initial condition of post-disturbance network is determined by both the type of disturbance under investigation and the duration of disturbance. In this research work, the loss of generation disturbance will be investigated.

For this type of disturbance, the initial condition in (4.2) can be computed from the initial operating condition of the load flow study. Assume that there are n-generators operating at equilibrium prior to disturbance. Generator x is suddenly dropped at $t=0^-$. The angles and velocities of generators can not change immediately. Hence, the velocities are equal to zero in (4.2). But angles with respect to center of inertia change because center of inertia changes due to the dropping of generator x. Then the first and second derivatives of $f_i(\underline{\theta})$ in (3.1) become

$$\dot{f}_i(\underline{\theta}) = 0.0$$

$$f_i(\underline{\theta}) = \nabla f(\underline{\theta})^T \cdot \dot{\tilde{\omega}} \qquad (4.8)$$

where $\dot{\tilde{\omega}}$ is an acceleration vector of generators which can be computed from the post-disturbance YBUS matrix and the rotor angles.

In consideration of the values of velocities at the two points and the nature of sine function, one can assume

$$\tilde{\omega}_i(t) = \sum_{k=1}^{\infty} (A_{ik} \sin(k\pi t))$$

$$\text{for } i=1, 2, \ldots, n \qquad (4.9)$$

and

$$\tilde{\omega}_i(0) = 0.0$$

$$\tilde{\omega}_i^{(3)}(1) = 0.0 \qquad \text{for } i=1, 2, \ldots, n$$

With this formulation, one can obtain the following approximations to the post-disturbance trajectory depending on the information utilized at the two points.

1. Utilizing rotor angles and velocities.

   Assume

$$\tilde{\omega}_i(t) = A_i \sin(\pi t)$$

$$0 \le t \le 1, \quad i=1, 2, \ldots, n \tag{4.10}$$

   Then

$$\theta_i(t) = \int_0^t \tilde{\omega}_i(s)ds + \theta_i^{cl}$$

$$= (A_i/\pi)\cos(\pi t) + (a_i/\pi) + \theta_i^{cl}$$

   where

$$A_i = 1/2\ \pi(\theta_i^u - \theta_i^{cl}) \tag{4.11}$$

2. Utilizing rotor angles, velocities, and accelerations

   Assume

$$\tilde{\omega}_i(t) = \sum_{k=1}^{3} A_{ik}\sin(k\pi t)$$

$$0 \le t \le 1, \qquad i=1, 2, \ldots, n$$

Then

$$\theta_i(t) = \sum_{k=1}^{3} (A_{ik}/k\pi)\cos(k\pi t)$$

$$+ \; 1/\pi \; (A_{i1} + A_{i2}/2 + A_{i3}/3) + \theta_i^{cl}$$

$$\tilde{\omega}_i(t) = \pi \sum_{k=1}^{3} kA_{ik}\cos(k\pi t)$$

and applying the boundary conditions, one can obtain

$$A_{i1} = 1/16[9\pi(\theta_i^u - \theta_i^{cl}) - 1/\pi f_i(\theta^{cl})/M_i]$$

$$A_{i2} = 1/4\pi(f_i(\theta^{cl})/M_i$$

$$A_{i3} = 3/16[1/\pi f_i(\theta^{cl})/M_i - \pi(\theta_i^u - \theta_i^{cl})] \qquad (4.12)$$

3. Utilizing rotor angles, velocities, accelerations, and derivative of accelerations.

Assume

$$\tilde{\omega}_i(t) = \sum_{k=1}^{5} A_{ik}\sin(k\pi t)$$

$$0 \le t \le 1 \quad \text{for } i=1, 2, \ldots\ldots, n$$

Then

$$\theta_i(t) = -1/\pi \sum_{k=1}^{5} (A_{ik}/k)\cos(k\pi t)$$

$$+ 1/\pi \sum_{k=1}^{5} (A_{ik}/k) + \theta_i^{cl}$$

$$\tilde{\omega}_i(t) = \pi \sum_{k=1}^{5} (kA_{ik})\cos(k\pi t)$$

$$\tilde{\omega}_i^{(2)}(t) = 0.0$$

$$\tilde{\omega}_i^{(3)}(t) = -\pi^3 \sum_{k=1}^{5} (k^3 A_{ik})\cos(k\pi t)$$

By applying the conditions at the two points, one can obtain

$$A_{i1} = 75\pi/128\ (\theta_i^u - \theta_i^{cl}) - 17\alpha_i/192\pi - \beta_i/384\pi^3$$

$$A_{i2} = 1/3\pi\ \alpha_i + \beta_i/48\pi^3$$

$$A_{i3} = -75\pi/256\ (\theta_i^u - \theta_i^{cl}) + 39\alpha_i/128\pi + 3\beta_i/256\pi^3$$

$$A_{i4} = -\alpha_i/24\pi - \beta_i/96\pi^3$$

$$A_{i5} = 15\pi/256(\theta_i^u - \&hecli.) - 25\alpha_i/384\pi - 5\beta_i/768\pi^3$$

where

$$\alpha_i = \dot{\tilde{\omega}}_i(0)$$

$$\beta_i = \tilde{\omega}_i^{(3)}(0)$$

CHAPTER V. SWING IMPEDANCE LOCUS FOLLOWING A DISTURBANCE

The TEF Formulation for Monitoring the Out-of-Step Relay

System dynamic performance analysis following a large disturbance is not limited to the study of transient stability. It also includes the study of network parameters due to the response of the synchronous machines to the disturbance. The effects of the swings on the synchronous machines following the disturbance are reflected as changes of voltage at the load buses, power flows over transmission lines, and the apparent impedances seen by the out-of-step relays.

In the previous chapter we have developed a technique for obtaining an approximated trajectory of the post-disturbance system in order to avoid explicit solution of the system's differential equations. The next step in the analysis is to develop a procedure for obtaining the swing impedance locus during the first swing transient by applying the techniques developed in the previous chapters. By examining the swing impedance locus, one can better understand the effects of the swings on the out-of-step relaying system.

In the formulation of the transient energy function method, a power system is reduced to the internal nodes of the synchronous machines. As a result, the physical entity of all other buses of interest are lost.

In order to incorporate out-of-step relay monitoring into the procedure of transient stability analysis by the transient energy function method, one should have the system reduced to the terminal buses of the generators with key buses of interest retained. The system reduced to the

internal nodes of generators is used for the stability assessment by the transient energy function method for a given set of scenarios. In addition, the system reduced to the terminal buses of generators will be used for the purpose of monitoring and computing the physical quantities at the buses retained during the transient such as the voltages at the relay buses and power flows over the tie lines of interest.

The practical significance of this formulation is that it can be used to obtain the voltage profile at some important load buses as a by-product of rapid transient stability assessment because the system required can be obtained as an intermediate reduction in the course of obtaining the system reduced to the internal nodes of generators.

Calculation of the Apparent Impedance Seen by the Out-of-Step Relay

After the elimination of all the buses except for the generator terminal buses, and the buses connecting the transmission lines monitored by out-of-step relays, the system can be represented as shown in Figure 2. The synchronous machines in the system in Figure 2 are represented by constant voltage source behind a transient reactance.

The voltages at the retained buses need to be evaluated in order to compute the swing impedance. The network equation is given by

$$\mathbf{I} = \mathbf{Y}*\mathbf{V} \tag{5.1}$$

where

$\mathbf{I}$: nodal current vector.

$\mathbf{V}$: nodal voltage vector.

$\mathbf{Y}$: YBUS matrix reduced to the generator terminal

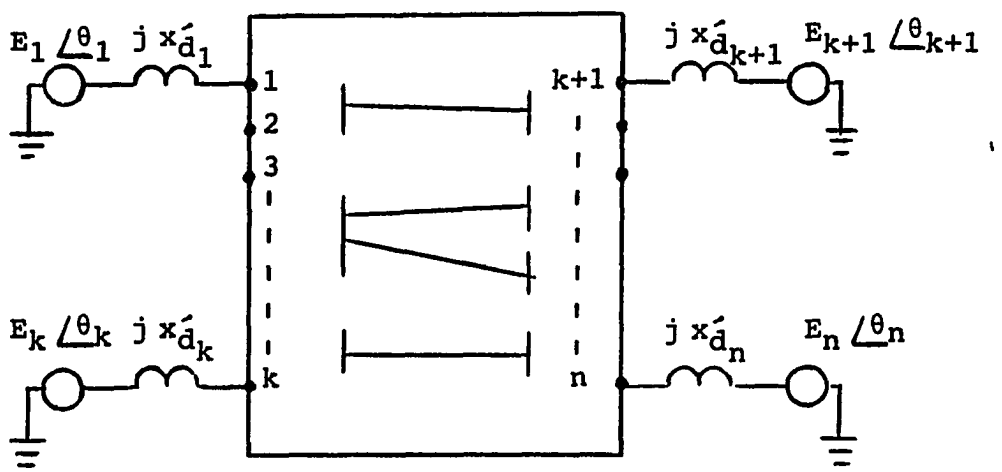

FIGURE 2. Network reduced to the generator terminal buses

buses with the relay buses retained.

Without loss of generality, one can assume that the first r components of nodal current and voltage vectors represent the values of the quantities at the relay buses. These components of the current vector are equal to zero because there is no source at these buses.

In order to incorporate the effects of the swings of the synchronous machines on the network equation in this formulation, one should convert the voltage source representation of the synchronous machines into the current source representation as shown in Figure 3

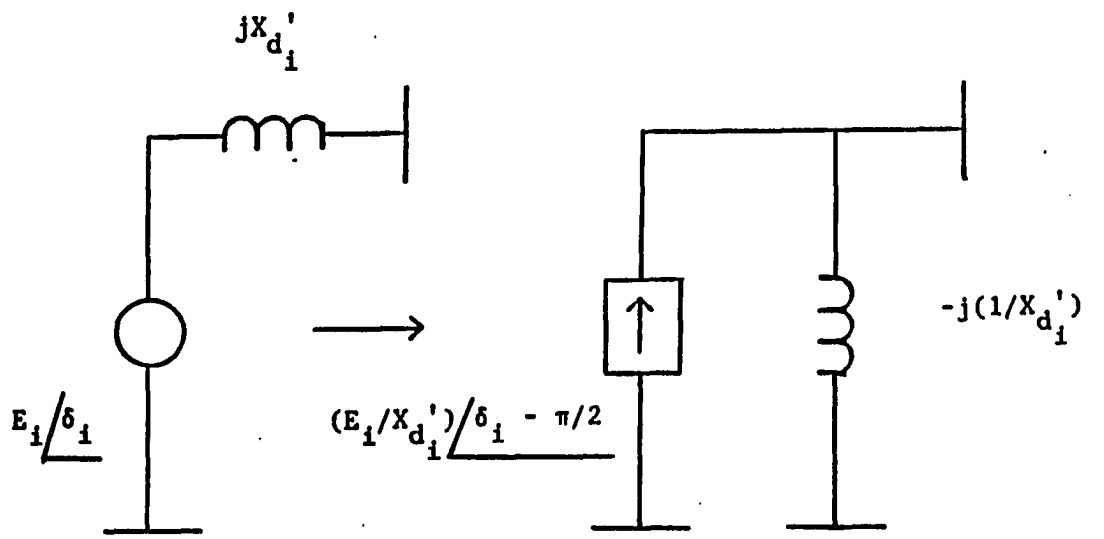

FIGURE 3. Current source representation of the synchronous machines

With this source conversion and with the shunt admittance being folded into the corresponding diagonal elements of the system YBUS matrix, the new network equation is given by

$$I = Y*V \tag{5.2}$$

where

I : constant magnitude current source vector with zero component for the non-generator terminal buses.

V : nodal voltage vector.

Y : modified system YBUS matrix.

The voltages at the relay buses are obtained by solving the network equation (5.2).

The apparent impedance seen by the out-of-step impedance at bus p in Figure 4 is given by.

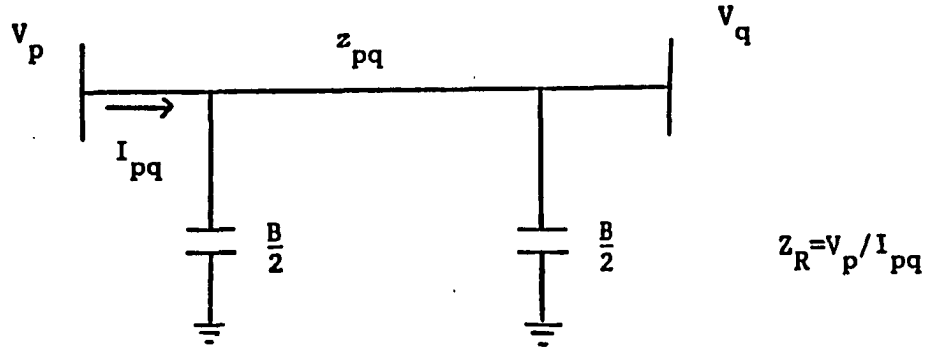

FIGURE 4. The transmission line monitored by out-of-step relay

$$Z_R = V_p / I_{pq} \tag{5.3}$$

where

$I_{pq} = (V_p - V_q)/z_{pq} + j(B/2)*V_p$

V_p, V_q : the voltage at bus p and q

z_{pq} : transmission line impedance

Procedure for Obtaining the Swing Impedance Locus

Using the techniques developed thus far, the swing impedance locus is obtained as follows:

Step 1: Compute the initial condition of the system prior to disturbance and admittance matrices YBUS of the post-disturbance network reduced to both the internal nodes of the generators and the generator terminal buses with the relay buses retained from the load flow study.

Step 2: Compute the condition of the system at the end of disturbance: $\underline{\theta}^{cl}$, $\underline{\tilde{\omega}}^{cl}$.

Step 3: Compute the post-disturbance stable equilibrium point $\underline{\theta}^{s2}$ and the controlling u.e.p. $\underline{\theta}^{u}$ for a given disturbance under investigation.

Step 4: Compute the transient energy margin ΔV from the system transient energy function and ΔV_{eq} from the two machine equivalent energy function.

Step 5: Compute the approximate trajectory of the post-disturbance network utilizing the conditions at the following points: a) the point where the disturbance is removed and b) the controlling u.e.p.

Step 6: Apply the energy-based criteria along the approximate trajectory of the post-disturbance network n order to determine the maximum swing angles $\underline{\theta}^m$.

Step 7: Starting from the values of $\underline{\theta}=\underline{\theta}^{cl}$ the voltage at the relay buses is obtained by solving the network equation (5.2). The current over the particular transmission line is calculated. Then, the apparent impedance seen by the out-of-step relay is calculated using equation (5.3). This procedure is carried out in step along the approximate trajectory determined in step 5 until $\underline{\theta}=\underline{\theta}^m$. This point on the system trajectory then provides the minimum apparent impedance.

Step 8: Draw the swing impedance thus obtained on the R-X diagram.

By comparing the swing impedance locus from the proposed procedure to the one obtained from time simulation, one can evaluate the efficiency and the accuracy of the techniques developed in dealing with practical power systems problems.

CHAPTER VI. RESULTS

Test System

The procedure developed in the previous chapters is tested on a 23-generator, 211-bus power system. That power system, shown in Figure 5, is a coherency-based dynamic equivalent derived from a large base case of the Florida Power & Light Company network using a special equivalencing computer program developed in [47]. This equivalent system was originally developed to investigate loss of generation disturbance by the transient energy function method in [29,35].

The Florida Power & Light Company network is connected to the Southern Company system by a number of tie lines. Figure 6 is a portion of the equivalent showing the four tie lines of interest between the Florida Power & Light Company network and the Southern Company system.[1] Heavy power was imported into Florida from the Southern company system over these tie lines. The loss of a large generator in Florida caused severe power and voltage swings over the (already) heavily loaded weak tie lines. The magnitude of such swings may be objectionable. For this reason out-of-step relays are often set to operate before loss of synchronism occurs, causing system separation.

In this research, the operation of out-of-step relay following loss of generation disturbance is analyzed by the techniques proposed in the

---

[1] Since this research project started, 500 KV transmission lines were added, which reduced this problem to a "second contingency" problem, i.e., it occurs after loss of 500 KV transmission lines.

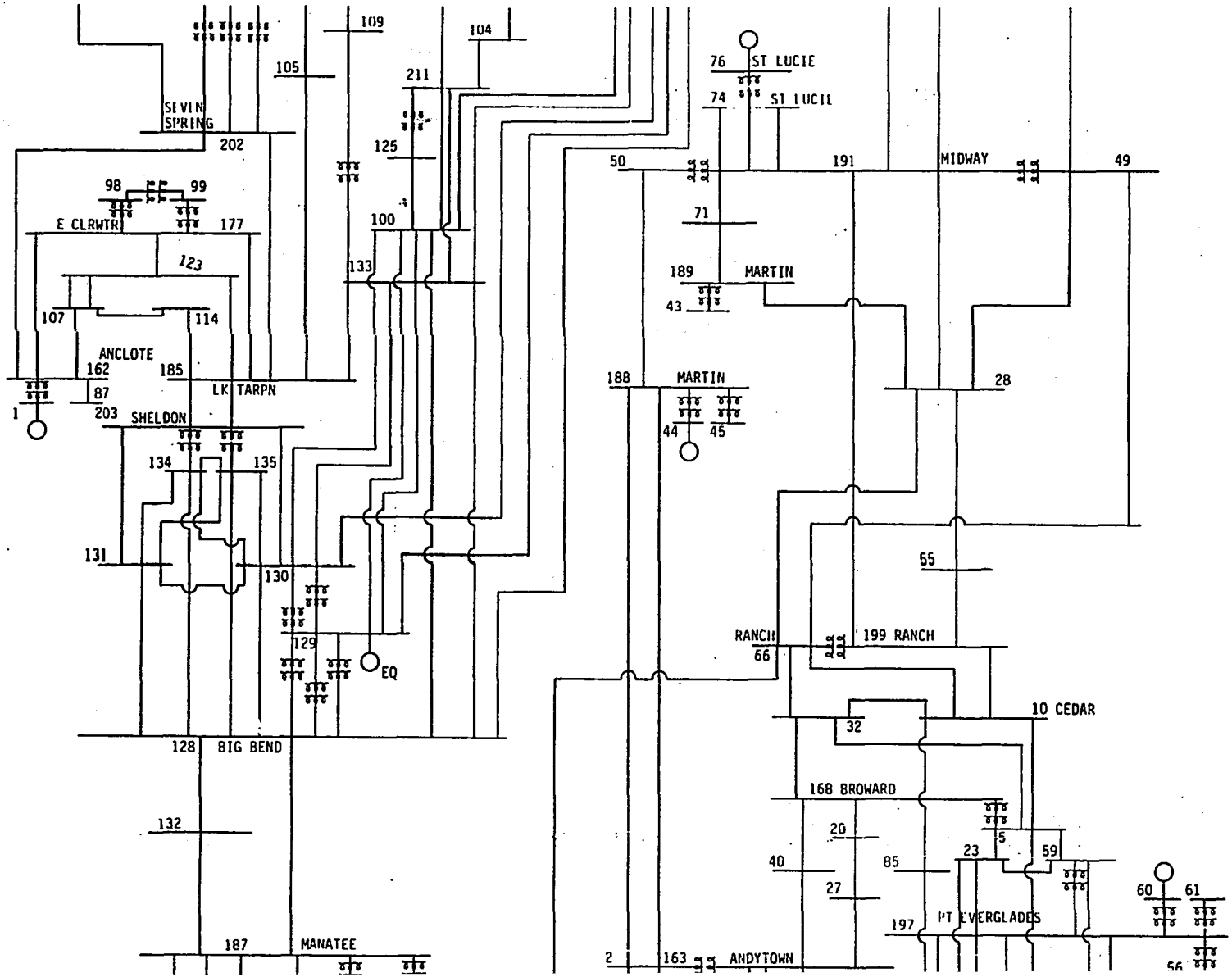
109
104
105
211
SEVIN
SPRING
202
76 ST LUCIE
74 ST LUCIE
125
50
191
MIDWAY
49
98
99
E CLRWTR
177
100
71
123
133
189
MARTIN
43
107
114
ANCLOTE
162
185
LK TARPN
87
203
1
SHELDON
188
MARTIN
28
44
45
134
135
131
55
130
129
EQ
RANCH
66
199 RANCH
10 CEDAR
32
128
BIG BEND
168 BROWARD
132
20
5
40
23
59
85
27
60
61
197
PT EVERGLADES
187
MANATEE
2
163
ANDYTOWN
56

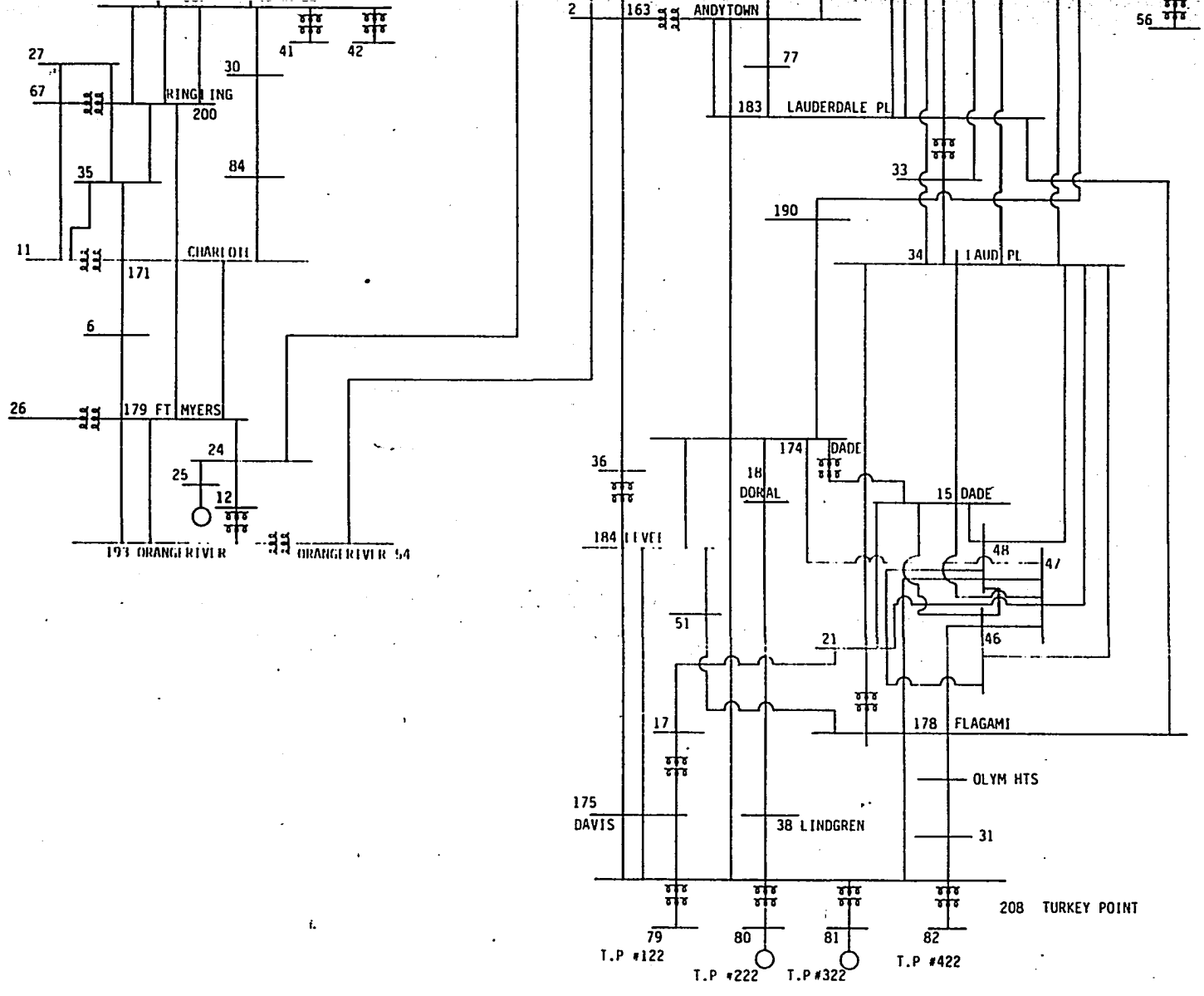

FIGURE 5. 23-generator system

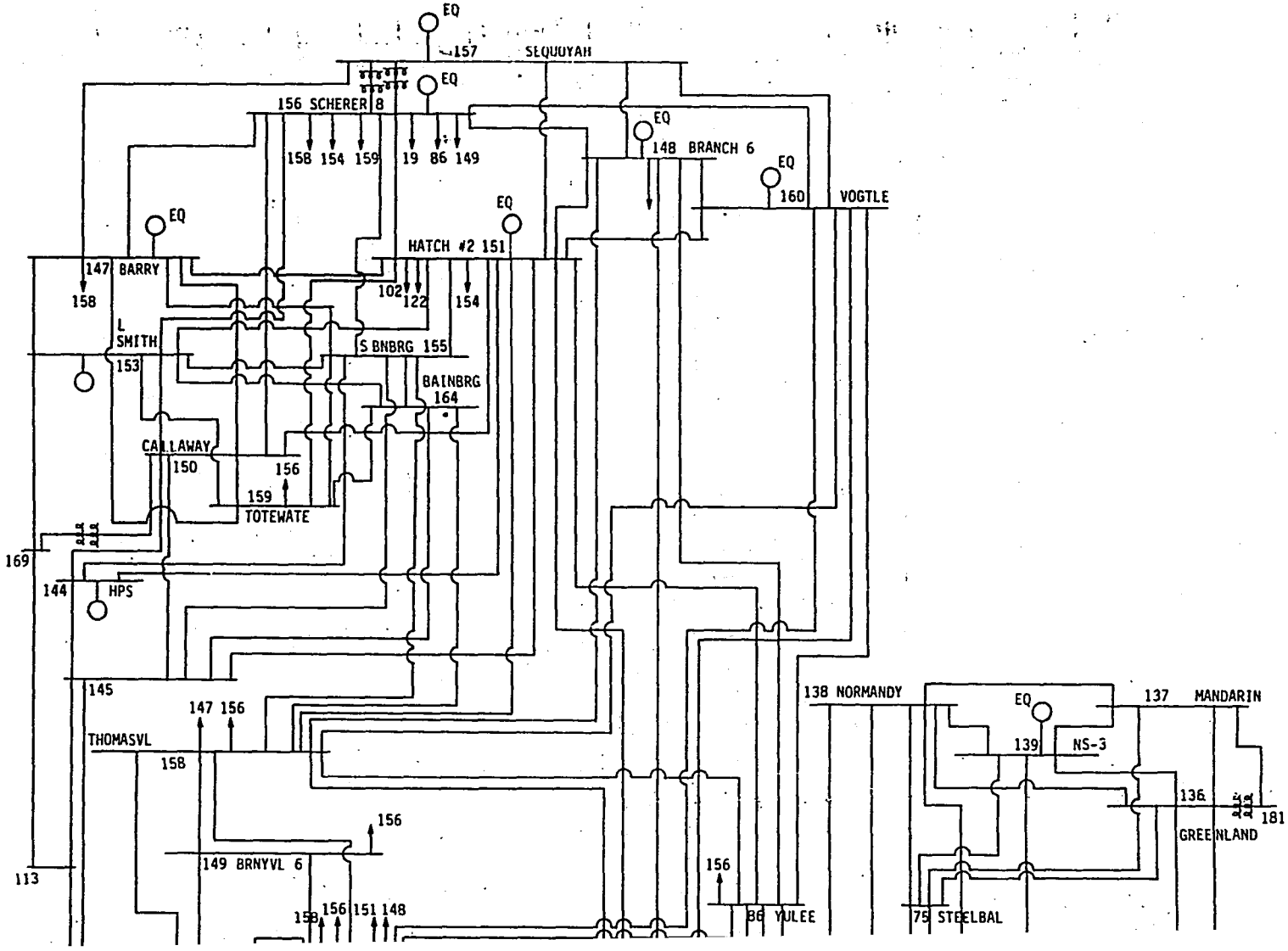
EQ
157 SEQUOYAH
EQ
156 SCHERER 8
158 154 159 19 86 149
EQ
148 BRANCH 6
EQ
160 VOGTLE
EQ
EQ
HATCH #2 151
147 BARRY
158
102 122 154
L SMITH
153
S BNBRG 155
BAINBRG 164
CALLAWAY 150
156
159 TOTEWATE
169
144 HPS
145
147 156
THOMASVL
158
156
149 BRNYVL 6
113
156 151 148
86 YULEE
156
138 NORMANDY
EQ
137 MANDARIN
139 NS-3
136
181
GREENLAND
75 STEELBAL

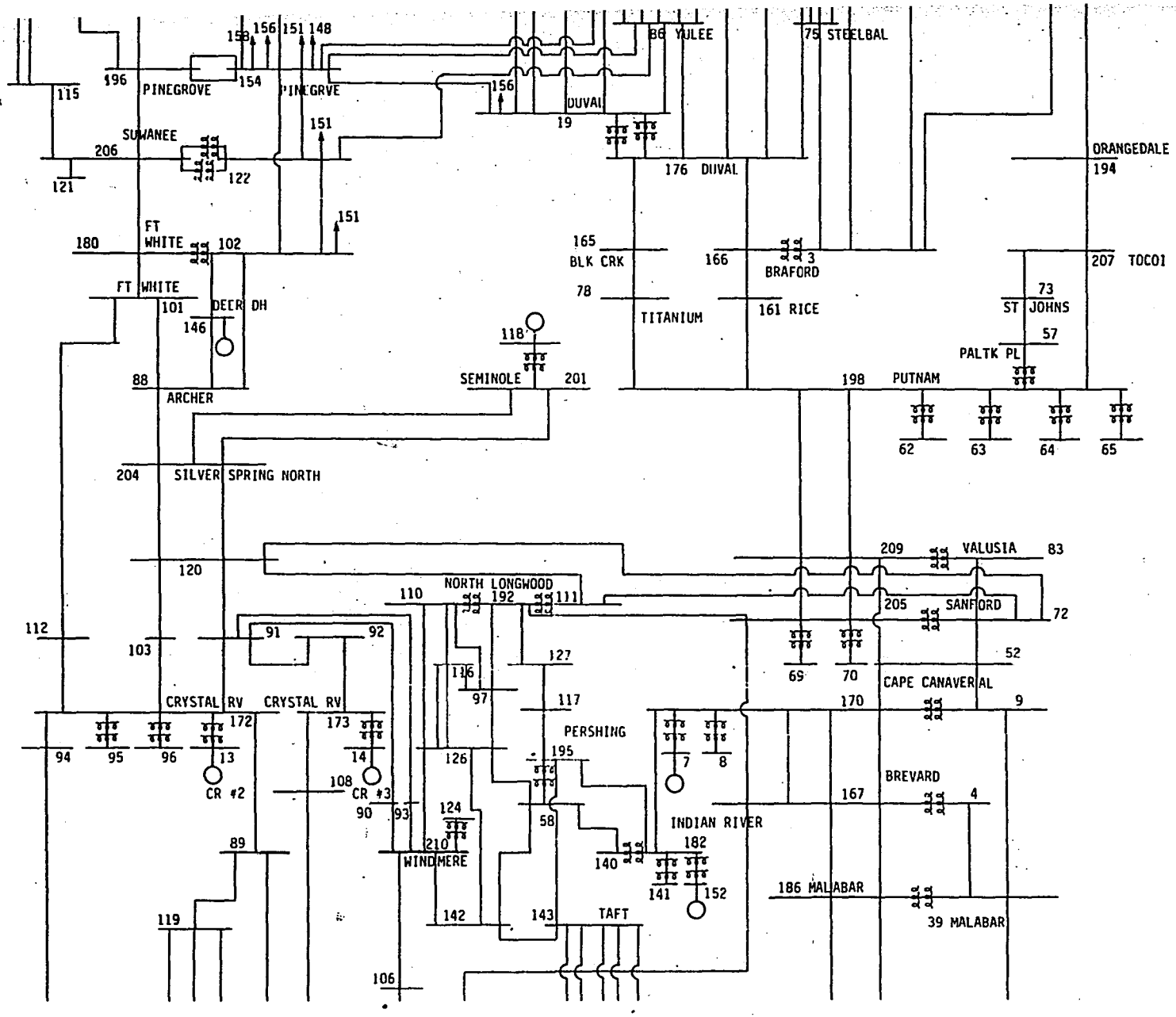

Figure 5 (continued)

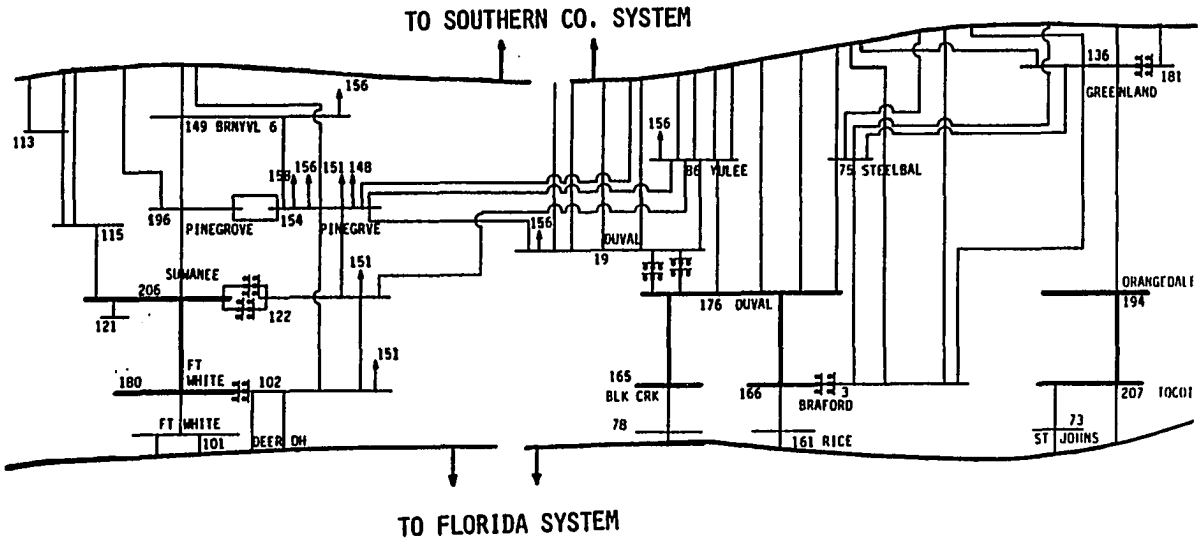

FIGURE 6. Portion of the Florida Power & Light Network showing the four tie lines of interest

previous chapters. For the purpose of verification of the proposed procedure, the swing impedance locus was obtained by time simulation, using the Philadelphia Electric Company Transient Stability Program.

The generator data and initial conditions for the base case are given in Table 1.

Evaluation

The following loss of generator disturbances were investigated in the 23-generator, 211-bus system:

- Loss of 880 Mw of generation at St. Lucie (generator no. 8)
- Loss of 820 Mw of generation at Crystal River (generator no. 4)
- Loss of 980 Mw of generation at St. Lucie (generator no. 8)
- Loss of 920 Mw of generation at Crystal River (generator no. 4)
- Loss of 1080 Mw of generation at St. Lucie (generator no. 8)
- Loss of 1020 Mw of generation at Crystal River (generator no. 4)

The first two cases are base cases that represent the Florida Power & Light Company network of 4000 Mw loading and were used to investigate transient stability by the transient energy function method in [29,35]. The remaining four cases are those obtained by changing the level of generation lost. For these modified cases, generation shift from the Southern system into the Florida system was made so that the load demand could be met in the pre-disturbance conditions.

The transient stability assessment by the transient energy function method [29] showed that all the cases were stable. These agreed with the results obtained with a conventional transient stability program. The

TABLE 1. Generator data and initial conditions of base case

Generator number	Generator Parameters[a]		Initial conditions		
				Internal Voltages	
	H (Mω/MVA)	X'_d (pu)	P_{mo}[a] (pu)	E (pu)	δ (degrees)
1	13.60	0.0429	2.500	1.0067	-38.54
2	12.26	0.0581	3.000	1.0245	-37.56
3	13.50	0.0438	4.705	1.0561	-28.83
4	30.77	0.0383	8.200	1.0720	-24.46
5	13.97	0.0592	3.000	1.0514	-49.05
6	26.48	0.0401	3.000	1.0022	-49.94
7	12.26	0.0581	2.893	1.0150	-52.44
8	33.20	0.0437	8.800	1.0572	-41.99
9	12.26	0.0581	3.600	1.0004	-46.91
10	30.67	0.0558	6.700	1.0729	-47.76
11	26.48	0.0354	2.900	1.0159	-25.58
12	55.37	0.0142	9.418	1.0244	-43.32
13	22.74	0.0368	1.534	0.9982	-22.78
14	6.31	0.1062	1.251	1.0013	-9.97
15	8.16	0.1182	0.768	0.9955	-27.06
16	87.51	0.0086	25.100	1.0552	10.53
17	30.34	0.0241	5.000	1.0368	-0.58
18	72.80	0.0193	15.790	1.0063	-3.20
19	10.34	0.0758	2.098	1.0231	-39.60
20	8.33	0.0795	1.500	1.0642	-5.32
21	194.85	0.0033	45.440	1.0071	-3.18
22	3996.00	0.0012	1.313	1.0441	-4.00
23	95.31	0.0159	9.120	1.0536	9.35

[a]On a 100-MVA base.

mode of disturbance for the cases studied was identical.

Tables 2 and 3 show the stable equilibrium point and the controlling u.e.p. of post-disturbance network. Using the procedure developed in the previous chapters, the transient energy margin is used to compute the corresponding minimum apparent swing impedance along the approximated trajectory of the post-disturbance network. The results are compared with the swing impeadnce locus obtained by time simulation.

Criteria for evaluation of the proposed technique

In the process of evaluation, the following results are checked against those from time simulation.

- The rotor angles of the various machines at maximum angles $\underline{\theta}^m$, i.e., at minimum apparent impedance seen by the out-of-step relay.
- The two kinds of trajectory approximations used: i) linear approximation, and ii) the Fourier series approximation. For the Fourier series approximations, the three different approximations developed in the Chapter IV were used for the purpose of comparison and improvement.
- The swing impedance locus obtained with the proposed energybased criteria and trajectory approximations.

In Tables 4 and 5 the rotor angles are given at $\underline{\theta}^m$ obtained both from time simulation and from the approximated trajectories by the two energy-based

TABLE 2. The stable equilibrium point and the controlling u.e.p. of the post-disturbance network when a generator at St. Lucie station is lost

gen. no.	Generation lost					
	880 Mω		980 Mω		1080 Mw	
	θ_{s2}[a]	θ_{u}[a]	θ_{s2}[a]	θ_{u}[a]	θ_{s2}[a]	θ_{u}[a]
1	-44.05	-155.39	-42.25	-156.12	-40.88	-156.77
2	-43.73	-161.63	-41.96	-162.51	-40.66	-163.34
3	-26.73	-133.97	-24.97	-134.71	-23.64	-135.33
4	-16.59	-120.22	-14.72	-120.76	-13.28	-121.21
5	-63.18	-180.12	-61.33	-180.88	-59.98	-181.60
6	-72.14	-191.47	-70.33	-192.29	-69.03	-193.08
7	-70.72	-188.88	-68.91	-189.68	-67.59	-190.45
8	_[b]	_[b]	_[b]	_[b]	_[b]	_[b]
9	-61.91	-179.44	-60.08	-180.23	-58.76	-181.00
10	-53.98	-171.33	-52.13	-172.10	-50.80	-172.86
11	-28.44	-137.19	-26.82	-138.16	-25.59	-138.98
12	-50.31	-164.56	-48.48	-165.30	-47.11	-165.97
13	-19.25	22.74	-18.68	23.73	-18.26	24.49
14	0.18	33.41	0.55	34.18	0.82	34.77
15	-28.27	-136.51	-26.83	-137.94	-25.74	-139.08
16	26.10	51.22	26.24	51.71	26.33	52.07
17	10.11	26.93	10.00	27.01	9.87	27.02
18	17.88	45.82	18.17	46.77	18.40	46.97
19	-46.72	-165.94	-44.94	-166.80	-43.63	-167.62
20	4.06	33.89	4.35	34.55	4.56	35.04
21	9.62	22.77	9.17	22.47	8.72	22.13
22	1.24	6.76	1.13	6.21	1.06	6.24
23	21.23	39.56	21.21	39.76	21.16	39.87

[a]All angles measured in degree with respect to COI.
[b]The generator lost.

TABLE 3. The stable equilibrium point and the controlling u.e.p. of the post-disturbance network when a generator at Crystal River is lost

gen. no.	Generation lost					
	820 Mω		920 Mω		1020 Mw	
	θ^{s2a}	θ^{ua}	θ^{s2a}	θ^{ua}	θ^{s2a}	θ^{ua}
1	-56.47	-156.13	-55.80	-156.50	-55.40	-156.80
2	-44.49	-139.95	-43.70	-140.15	-43.21	-140.27
3	-38.43	-136.27	-37.70	-136.57	-37.30	-136.82
4	_b	_b	_b	_b	_b	_b
5	-58.64	-155.97	-57.85	-156.17	-57.37	-156.31
6	-60.87	-158.15	-60.04	-158.31	-59.52	-159.40
7	-60.84	-157.55	-60.01	-157.71	-59.49	-157.80
8	-37.54	-133.05	-36.67	-133.15	-36.12	-133.19
9	-52.34	-148.64	-51.51	-148.79	-50.98	-148.86
10	-44.57	-140.78	-43.72	-140.91	-43.18	-140.96
11	-39.74	-139.54	-39.04	-139.90	-38.65	-140.17
12	-56.87	-155.70	-56.15	-156.00	-55.75	-156.24
13	-20.48	14.57	-20.18	15.09	-20.00	15.42
14	-1.12	31.00	-0.91	31.45	-0.78	31.74
15	-37.62	-138.82	-36.95	-139.25	-36.56	-139.54
16	25.79	49.22	25.87	49.49	25.92	49.66
17	9.95	25.18	9.82	25.13	9.67	25.01
18	17.41	43.26	17.62	43.65	17.76	43.92
19	-47.78	-144.71	-46.98	-144.90	-46.49	-145.03
20	3.12	31.58	3.29	31.96	3.40	32.10
21	9.58	21.42	9.14	21.03	8.70	20.61
22	1.50	5.68	1.47	5.70	1.46	5.72
23	21.06	37.70	21.01	37.74	20.94	37.72

[a]All angles measured in degree with respect to COI.
[b]The generator lost.

TABLE 4. Maximum swing angles: St. Lucie 880 Mw lost

gen.	time simulation no.	linear		approximation series					
				1-term		3-term		5-term	
		θ^{m_a}	θ^{m_b}	θ^{m_a}	θ^{m_b}	θ^{m_a}	θ^{m_b}	θ^{m_a}	θ^{m_b}
1	-70.5	-64.8	-69.8	-64.6	-69.9	-70.1	-70.3	-70.8	-71.3
2	-67.9	-63.1	-68.6	-62.9	-68.7	-74.3	-74.4	-76.8	-77.3
3	-50.3	-48.1	-52.9	-47.9	-52.9	-53.0	-53.2	-53.7	-54.1
4	-43.8	-36.5	-41.1	-36.3	-41.1	-41.0	-41.2	-41.5	-41.9
5	-91.3	-77.0	-82.8	-76.8	-82.8	-89.0	-89.2	-91.9	-92.4
6	-100.7	-82.5	-88.6	-82.3	-88.6	-100.5	-100.7	-105.2	-105.7
7	-96.2	-81.7	-87.7	-81.5	-87.7	-98.4	-98.7	-102.8	-103.3
8	-[c]	-[c]	-[c]	-[c]	-[c]	-[c]	-[c]	-[c]	-[c]
9	-86.7	-73.1	-79.0	-72.9	-79.0	-86.7	-86.9	-90.2	-90.7
10	-75.1	-65.3	-71.2	-65.1	-71.2	-74.9	-75.1	-77.0	-77.5
11	-53.9	-50.9	-55.4	-50.4	-55.4	-55.7	-55.9	-56.4	-56.8
12	-77.4	-69.8	-75.1	-69.6	-75.1	-76.5	-76.6	-77.7	-78.2
13	-22.7	-4.8	-3.2	-4.8	-3.2	-3.5	-3.4	-3.4	-3.3
14	-0.9	10.4	11.7	10.4	11.7	12.0	12.0	12.2	12.3
15	-49.7	-51.9	-56.6	-51.7	-56.6	-56.8	-57.0	-57.4	-57.8
16	26.5	32.9	34.0	32.9	34.0	34.2	34.3	34.4	34.5
17	11.0	14.5	15.2	14.5	15.2	15.4	15.4	15.6	15.6
18	18.6	25.8	26.9	25.7	26.9	27.2	27.2	27.4	27.5
19	-70.9	-66.5	-72.1	-66.3	-72.1	-77.8	-77.9	-80.4	-80.8
20	3.6	12.9	14.1	12.9	14.1	14.4	14.4	14.6	14.7
21	10.8	12.8	12.4	12.8	13.4	13.5	13.6	13.7	13.7
22	2.9	1.8	2.1	1.8	2.1	2.3	2.3	2.2	2.2
23	21.8	21.3	21.3	21.3	21.3	21.6	21.6	21.6	21.6

[a]Based on the system total energy criterion.
[b]Based on the two machine equivalent energy criterion.
[c]The generator lost.

TABLE 5. Maximum swing angles: Crystal River 820 Mw lost

time simulation	linear		approximation series					
			1-term		3-term		5-term	
gen. no.	θ^{m_a}	θ^{m_b}	θ^{m_a}	θ^{m_b}	θ^{m_a}	θ^{m_b}	θ^{m_a}	θ^{m_b}
1 -81.5	-66.2	-75.6	-66.1	-75.5	-72.6	-84.6	-74.0	-87.6
2 -64.2	-58.1	-66.6	-57.9	-66.5	-55.6	-66.7	-53.8	-66.6
3 -61.3	-49.9	-58.9	-49.8	-58.9	-55.1	-66.6	-56.0	-69.2
4 _[c]	_[c]	_[c]	_[c]	_[c]	_[c]	_[c]	_[c]	_[c]
5 -81.9	-71.3	-80.1	-71.2	-80.0	-66.6	-78.0	-63.8	-77.2
6 -85.3	-74.1	-82.9	-74.0	-82.8	-68.9	-80.3	-65.9	-79.3
7 -84.6	-73.9	-82.7	-73.8	-82.6	-68.9	-80.3	-65.9	-79.3
8 -61.1	-50.7	-59.3	-50.6	-59.2	-45.2	-56.4	-42.2	-55.3
9 -75.8	-65.4	-74.1	-65.3	-74.0	-59.9	-71.2	-56.8	-70.1
10 -66.8	-57.7	-66.4	-57.6	-66.3	-51.93	-63.2	-48.7	-62.0
11 -63.7	-52.4	-61.53	-52.3	-61.5	-51.1	-62.9	-49.7	-63.3
12 -78.7	-68.5	-77.58	-68.4	-77.5	-67.3	-79.0	-65.8	-79.5
13 -21.8	-6.7	-4.5	-6.8	-4.5	-8.8	-5.6	-9.9	-6.4
14 .7	10.0	12.2	10.0	12.2	8.2	11.0	7.1	10.5
15 -57.5	-53.7	-62.6	-53.6	-62.5	-51.2	-62.7	-49.3	-62.7
16 30.0	32.7	34.4	32.6	34.4	31.7	33.9	31.1	33.8
17 12.2	14.2	15.4	14.2	15.4	13.4	15.1	13.2	14.9
18 20.3	25.4	27.2	25.3	27.2	24.2	26.7	23.5	26.4
19 -67.7	-61.6	-70.3	-61.5	-70.2	-59.5	-70.7	-57.7	-70.8
20 5.6	12.6	14.6	12.6	14.6	11.0	13.6	10.2	13.2
21 11.4	12.6	13.5	12.6	13.5	12.1	13.3	11.8	13.2
22 3.5	1.7	2.1	1.7	2.1	1.6	2.1	1.4	2.0
23 24.1	25.8	27.0	25.8	27.0	25.1	26.7	24.7	26.6

[a]Based on the system total energy criterion.
[b]Based on the two machine equivalent energy criterion.
[c]The generator lost.

criteria developed in Chapter III for the loss of 880 Mw of generation at St. Lucie station and the loss of 820 Mw of generation at Crystal River station, respectively. The apparent impedances are computed for the out-of-step relay on the Ft.White-Suwanee line at the Ft. White bus.

By examining the data given in Tables 4 and 5, the following obervations can be made:

- The rotor angles of $\underline{\theta}^m$ obtained by the linear approximation to the trajectory are very close to those of $\underline{\theta}^m$ obtained by the 1-term approximation.
- The 3-term and the 5-term series approximations to the system trajectory give similar values of $\underline{\theta}^m$.
- The two energy-based criteria provide good results when the 3-term and the 5-term series approximations are used. While both criteria provide similar results for the case of loss of 880 Mw of generation at St. Lucie station, the criterion based on the two machine equivalent energy give better results for the case of loss of 820 Mw of generation at Crystal River station.
- When the linear or the 1-term approximation to the trajectory is used, the criterion based on the two machine equivalent energy gives better agreement with time simulation than when the criterion based on the total system energy is used.

When the level of generation lost is increased by 100 Mw and 200 Mw at both of the generation stations, the rotor angles at $\underline{\theta}^m$ are given in Tables 6-9.

TABLE 6. Maximum swing angles: St. Lucie 980 Mw lost

time simulation		linear		approximation series					
				1-term		3-term		5-term	
gen.	no.	θ^{ma}	θ^{mb}	θ^{ma}	θ^{mb}	θ^{ma}	θ^{mb}	θ^{ma}	θ^{mb}
1	-72.4	-66.0	-70.6	-66.0	-70.7	-71.3	-74.5	-71.9	-75.1
2	-70.0	-64.5	-70.0	-64.5	-70.0	-76.1	-79.4	-78.6	-82.0
3	-51.9	-49.5	-53.8	-49.5	-53.9	-54.3	-57.3	-54.8	-57.8
4	-45.6	-37.4	-41.7	-37.4	-41.8	-41.8	-44.8	-42.2	-45.2
5	-93.5	-77.8	-83.1	-77.8	-83.2	-90.3	-93.8	-93.2	-96.7
6	-103.2	-83.2	-88.8	-83.2	-88.9	-102.2	-105.8	-106.9	-110.5
7	-98.2	-82.4	-87.9	-82.4	-88.1	-99.9	-103.5	-104.4	-107.9
8	-[c]	-[c]	-[c]	-[c]	-[c]	-[c]	-[c]	-[c]	-[c]
9	-88.6	-73.8	-79.2	-73.7	-79.3	-87.9	-91.6	-91.4	-94.9
10	-76.6	-65.9	-71.4	-65.9	-71.5	-75.7	-79.3	-77.7	-81.4
11	-55.8	-52.2	-56.6	-52.2	-56.7	-57.2	-60.2	-57.6	-60.7
12	-79.3	-70.1	-75.8	-70.9	-75.9	-77.7	-80.9	-78.8	-82.1
13	-22.7	-2.1	-0.8	-2.1	-0.7	-1.1	-0.2	-1.1	-0.2
14	-0.8	12.3	13.5	12.3	13.5	13.8	14.5	13.9	14.7
15	-51.2	-54.0	-58.3	-53.9	-58.4	-58.7	-61.6	-59.1	62.1
16	26.4	34.2	35.1	34.2	35.1	35.4	36.0	35.6	36.2
17	10.9	15.1	15.7	15.1	15.7	15.9	16.4	16.1	16.5
18	18.9	27.3	28.3	27.3	28.3	28.6	29.3	28.8	29.4
19	-72.7	-67.9	-73.0	-67.9	-73.1	-79.6	-82.9	-82.2	-85.6
20	3.7	14.6	15.7	14.6	15.7	15.9	16.6	16.1	16.8
21	10.5	12.9	13.4	12.9	13.4	13.6	13.9	13.7	14.0
22	3.0	1.6	1.9	1.6	1.9	2.1	2.3	2.0	2.2
23	21.6	26.8	27.5	26.8	27.5	27.7	28.2	27.9	28.3

[a]Based on the system total energy criterion.
[b]Based on the two machine equivalent energy criterion.
[c]The generator lost.

TABLE 7. Maximum swing angles: Crystal River 920 Mw lost

time simulation		linear		approximation series					
				1-term		3-term		5-term	
gen.	no.	θ^{ma}	θ^{mb}	θ^{ma}	θ^{mb}	θ^{ma}	θ^{mb}	θ^{ma}	θ^{mb}
1	-84.5	-67.7	-77.7	-67.7	-77.8	-75.5	-87.9	-77.0	-91.2
2	-66.4	-59.7	-68.7	-59.7	-68.8	-57.4	-69.0	-55.3	-69.0
3	-64.0	-51.6	-61.1	-51.6	-61.2	-57.9	-69.8	-59.0	-72.6
4	-[c]	-[c]	-[c]	-[c]	-[c]	-[c]	-[c]	-[c]	-[c]
5	-84.4	-72.8	-82.2	-72.8	-82.3	-67.9	-80.0	-64.8	-79.2
6	-87.9	-75.7	-85.0	-75.7	-85.1	-70.2	-82.2	-66.8	-81.1
7	-87.1	-75.5	-84.7	-75.5	-84.8	-70.0	-82.0	-66.6	-80.8
8	-63.7	-52.2	-61.3	-52.2	-61.4	-46.4	-58.2	-42.9	-57.0
9	-78.2	-66.9	-76.1	-66.9	-76.2	-61.2	-73.1	-57.6	-71.9
10	-69.2	-59.2	-68.4	-59.2	-68.5	-53.1	-65.0	-49.4	-63.6
11	-66.2	-54.2	-63.9	-54.2	-64.0	-53.2	-65.5	-51.5	66.0
12	-81.1	-70.1	-79.7	-70.1	-79.8	-69.2	-81.5	-67.6	-82.1
13	-21.3	-4.5	-2.3	-4.5	-2.3	-6.7	-3.8	-7.9	-4.4
14	1.5	12.0	14.2	12.0	14.2	10.0	12.8	8.8	12.2
15	-59.6	-55.9	-65.2	-55.9	-65.3	-53.5	-65.5	-51.4	-65.5
16	31.0	33.9	35.6	33.9	35.6	32.9	35.2	32.2	34.9
17	12.5	14.8	15.9	14.8	15.9	14.1	15.6	13.7	15.5
18	21.2	26.8	28.7	26.8	28.7	25.6	28.0	24.9	27.8
19	-69.9	-63.3	-72.4	-63.3	-72.5	-61.4	-73.1	-59.4	-73.2
20	6.5	14.2	16.2	14.2	16.3	12.5	15.1	11.5	14.7
21	11.3	12.7	13.6	12.7	13.6	12.1	13.4	11.8	13.2
22	2.8	1.7	2.1	1.7	2.1	1.6	2.2	1.4	2.1
23	24.6	26.5	27.7	26.5	27.7	25.8	27.5	25.4	27.3

[a]Based on the system total energy criterion.
[b]Based on the two machine equivalent energy criterion.
[c]The generator lost.

TABLE 8. Maximum swing angles: St. Lucie 1080 Mw lost

gen.	time simulation no.	linear		approximation series					
				1-term		3-term		5-term	
		θ^{ma}	θ^{mb}	θ^{ma}	θ^{mb}	θ^{ma}	θ^{mb}	θ^{ma}	θ^{mb}
1	-74.7	-67.8	-72.3	-67.9	-72.4	-72.9	-75.9	-73.4	-73.5
2	-72.0	-66.5	-71.5	-66.6	-71.6	-78.3	-81.4	-80.9	-80.9
3	-53.9	-51.3	-55.6	-51.4	-55.7	-55.9	-58.7	-56.3	-56.4
4	-47.9	-38.9	-43.1	-38.9	-43.1	-43.0	-45.8	-43.3	-43.4
5	-96.4	-79.3	-84.5	-79.4	-84.7	-92.1	-95.3	-94.9	-95.0
6	-106.3	-84.7	-90.2	-84.8	-90.3	-104.3	-107.7	-109.1	-109.3
7	-100.9	-83.9	-89.3	-83.9	-89.4	-101.9	-105.3	-106.5	-106.6
8	-[c]	-[c]	-[c]	-[c]	-[c]	-[c]	-[c]	-[c]	-[c]
9	-91.2	-75.1	-80.6	-75.2	-80.6	-89.7	-93.1	-93.1	-93.3
10	-78.7	-67.3	-72.7	-67.4	-72.8	-77.0	-80.4	-78.9	-79.0
11	-58.1	-54.3	-58.6	-54.3	-58.7	-58.9	-61.7	-59.3	-59.4
12	-81.8	-72.7	-77.5	-72.8	-77.6	-79.3	-82.4	-80.4	-80.5
13	-22.7	0.4	1.6	0.4	1.7	1.1	2.0	1.0	1.0
14	-0.7	14.2	15.2	14.2	15.2	15.4	16.1	15.6	15.6
15	-53.1	-56.4	-60.6	-56.5	-60.7	-60.8	-63.6	-61.1	-61.2
16	26.3	35.4	36.2	35.4	36.2	36.5	37.1	36.6	36.6
17	10.8	15.7	16.2	15.7	16.3	16.5	16.8	16.6	16.6
18	19.2	28.8	29.7	28.8	29.8	29.9	30.6	30.1	30.1
19	-75.1	-70.0	-74.9	-70.1	-75.1	-81.9	-84.9	-84.4	-84.5
20	3.7	16.2	17.2	16.2	17.2	17.4	18.0	17.5	17.5
21	10.1	12.9	13.4	12.9	13.4	13.6	13.9	13.7	13.7
22	3.2	1.7	1.9	1.7	1.9	2.1	2.3	2.0	2.0
23	21.4	27.5	28.1	27.5	28.2	28.4	28.8	28.5	28.5

[a]Based on the system total energy criterion.
[b]Based on the two machine equivalent energy criterion.
[c]The generator lost.

TABLE 9. Maximum swing angles: Crystal River 1020 Mw lost

time simulation		linear		approximation series					
				1-term		3-term		5-term	
gen.	no.	θ_{max}[a]	θ_{max}[b]	θ_{max}[a]	θ_{max}[b]	θ_{max}[a]	θ_{max}[b]	θ_{max}[a]	θ_{max}[b]
1	-87.7	-70.2	-80.9	-70.2	-80.9	-78.9	-91.7	-80.7	-95.2
2	-68.9	-62.1	-71.8	-62.1	-71.8	-59.7	-71.9	-57.5	-71.9
3	-66.9	-54.0	-64.2	-54.0	-64.2	-61.3	-73.58	-62.6	-76.6
4	_c	_c	_c	_c	_c	_c	_c	_c	_c
5	-87.3	-75.2	-85.2	-75.2	-85.2	-69.9	-82.7	-66.5	-81.8
6	-91.0	-78.1	-88.0	-78.1	-88.0	-72.0	-84.8	-68.4	-83.6
7	-90.0	-77.8	-87.7	-77.8	-87.7	-71.8	-84.5	-68.2	-83.3
8	-66.8	-54.4	-64.1	-54.4	-64.1	-48.1	-60.6	-44.4	-59.4
9	-81.2	-69.2	-79.1	-69.3	-79.1	-62.9	-75.6	-59.2	-74.3
10	-72.1	-61.5	-71.3	-61.5	-71.3	-54.7	-67.4	-50.9	-66.0
11	-68.9	-56.8	-67.1	-56.9	-67.1	-55.8	-68.7	-54.1	-69.2
12	-83.9	-72.5	-82.8	-72.5	-82.8	-71.7	-84.6	-70.1	-85.3
13	-20.8	-2.4	-0.2	-2.4	-0.2	-4.8	-1.9	-6.0	-2.5
14	2.4	13.8	16.0	13.8	16.0	11.5	14.4	10.3	13.8
15	-61.6	-58.7	-68.7	-58.8	-68.7	-56.3	-68.9	-54.0	-68.9
16	32.0	35.1	36.9	35.1	36.9	34.0	36.4	33.4	36.1
17	12.8	15.3	16.5	15.3	16.5	14.6	16.2	14.2	16.0
18	22.0	28.3	30.2	28.3	30.2	27.0	29.5	26.2	29.2
19	-72.4	-65.7	-75.5	-65.8	-75.5	-63.7	-76.1	-61.7	-76.2
20	-7.4	15.8	17.8	15.8	17.8	13.9	16.6	12.9	16.1
21	11.2	12.7	13.7	12.7	13.7	12.2	13.4	11.8	13.3
22	3.0	1.7	2.2	1.7	2.2	1.7	2.3	1.4	2.1
23	25.2	27.2	28.5	27.2	28.5	26.5	28.2	26.0	28.0

[a]Based on the system total energy criterion.
[b]Based on the two machine equivalent energy criterion.
[c]The generator lost.

The comparison of maximum swing angles

By examining the changes of the rotor angles at $\underline{\theta}^m$, the following observations can be made:

- For the case of loss of generation at St. Lucie station the rotor angles at $\underline{\theta}^m$ of the critical machines change about 2-3 % as the level of generation lost is increased by 100 Mω. However, for the case of loss of generation at Crystal River station, the rotor angles at $\underline{\theta}^m$ of the critical machines change 3-4.5 % as the level of generation lost is increased by 100 Mω.
- While the rotor angles at $\underline{\theta}^m$ of the critical machines change, those of the non-critical machines do not change.
- While the rotor angles at $\underline{\theta}^m$ of the critical machines determined by the proposed technique compare well with those obtained with time simulation, some of the non-critical machines are off by some extent.

The swing impedance locus was obtained by the procedure proposed in Chapter V using the two energy-based criteria along the approximated trajectory. For the two base cases, the results are given in Figures 7-21. For each case the results with the proposed procedure are given together with time simulation for easy comparison.

The comparison of minimum apparent impedance seen by the out-of-step relay

The results displayed in Figures 7-21 show the followings:

- Both energy-based criteria give values of minimum apparent impedance seen by the out-of-step relay which compare well with the values obtained by time simulation. This is shown by the

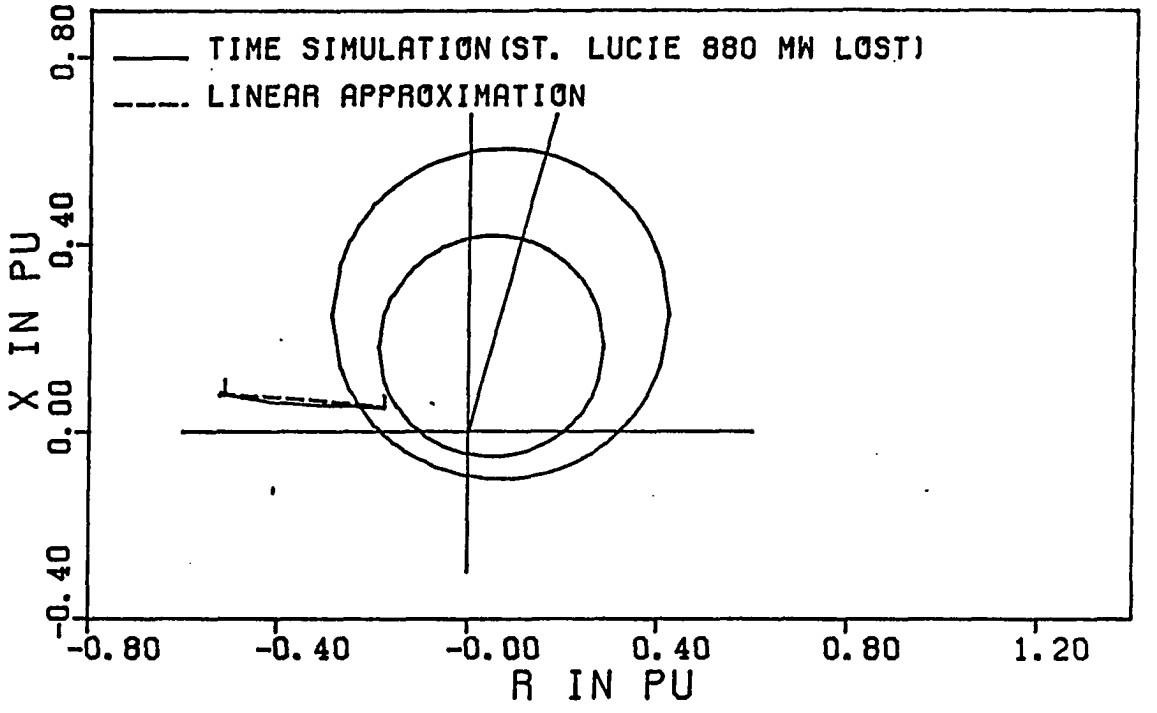

FIGURE 7. Loss of 880 Mw of generation at St. Lucie: linear approximation based on the system energy

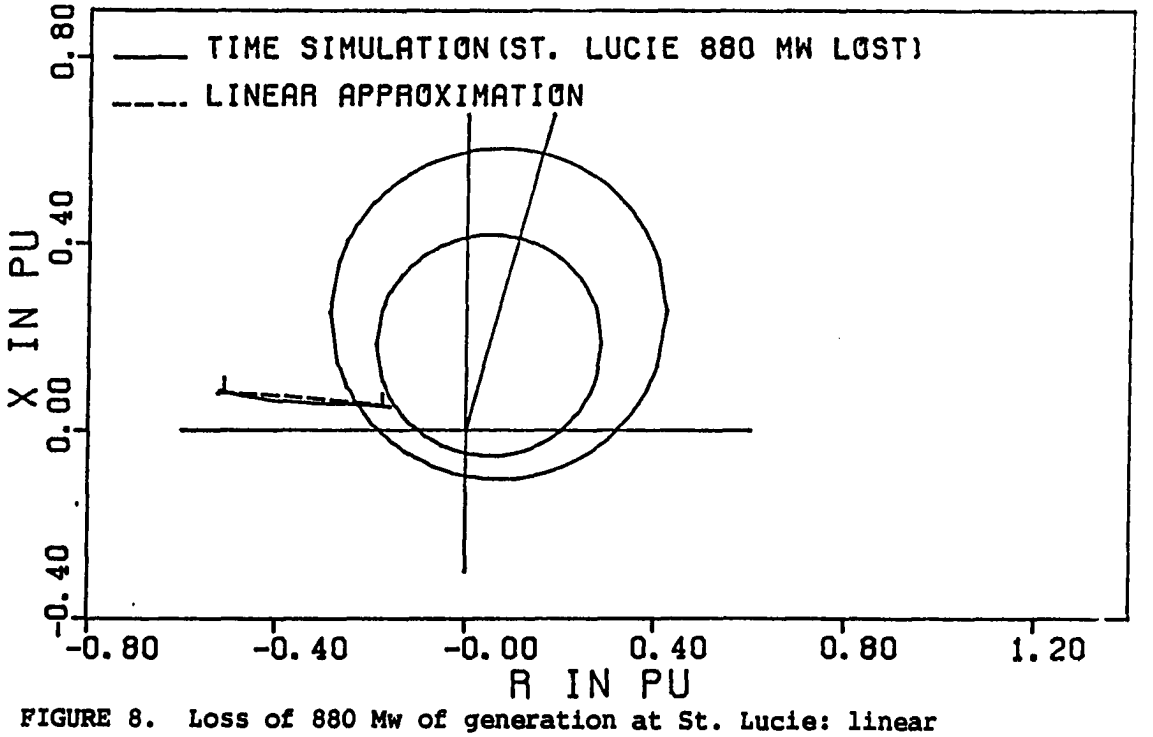

FIGURE 8. Loss of 880 Mw of generation at St. Lucie: linear approximation based on the equivalent energy

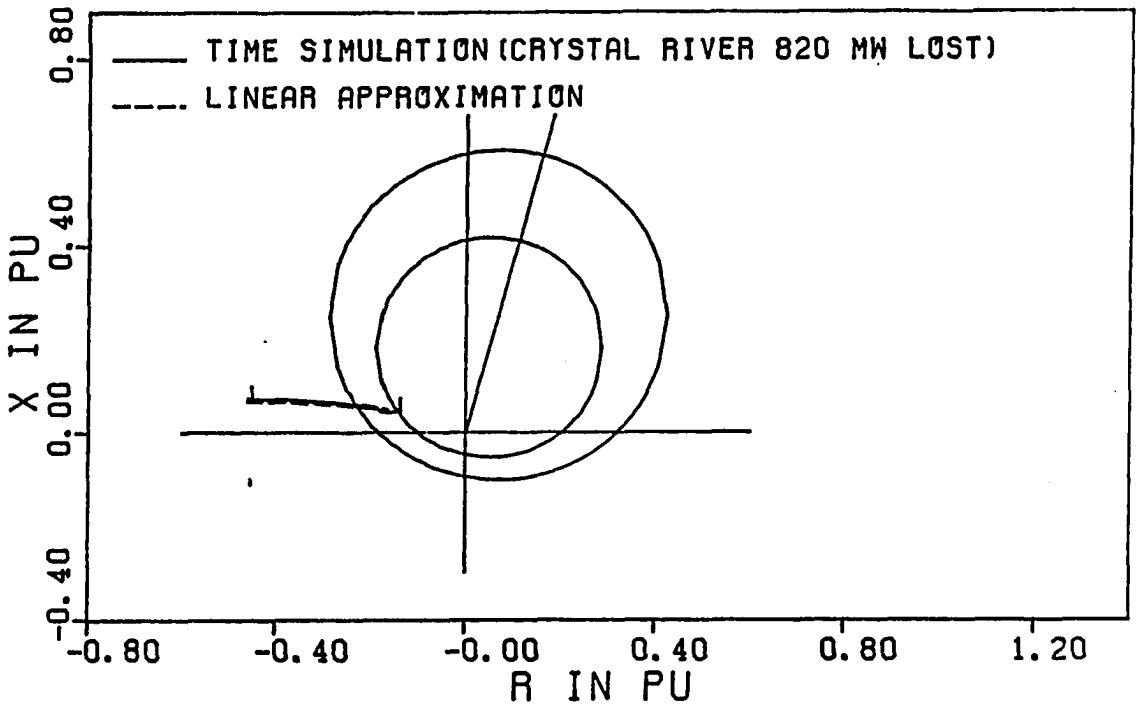

FIGURE 9. Loss of 820 Mw of generation at Crystal River: linear approximation based on the system energy

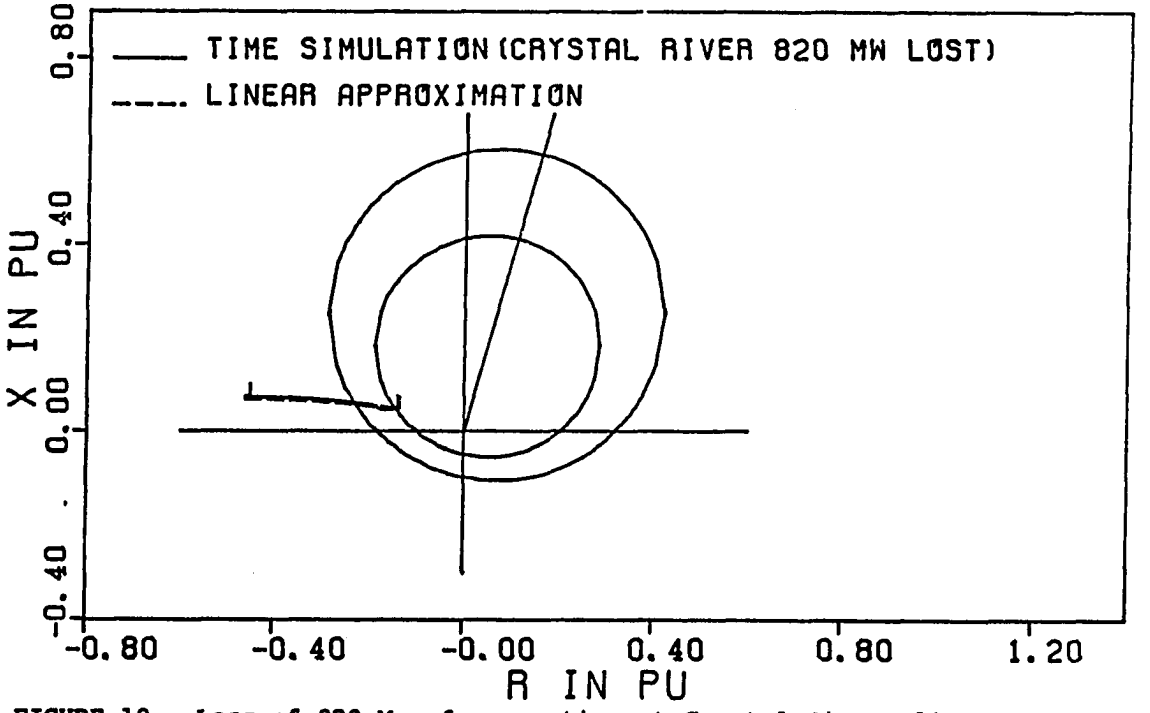

FIGURE 10. Loss of 820 Mw of generation at Crystal River: linear approximation based on the equivalent energy

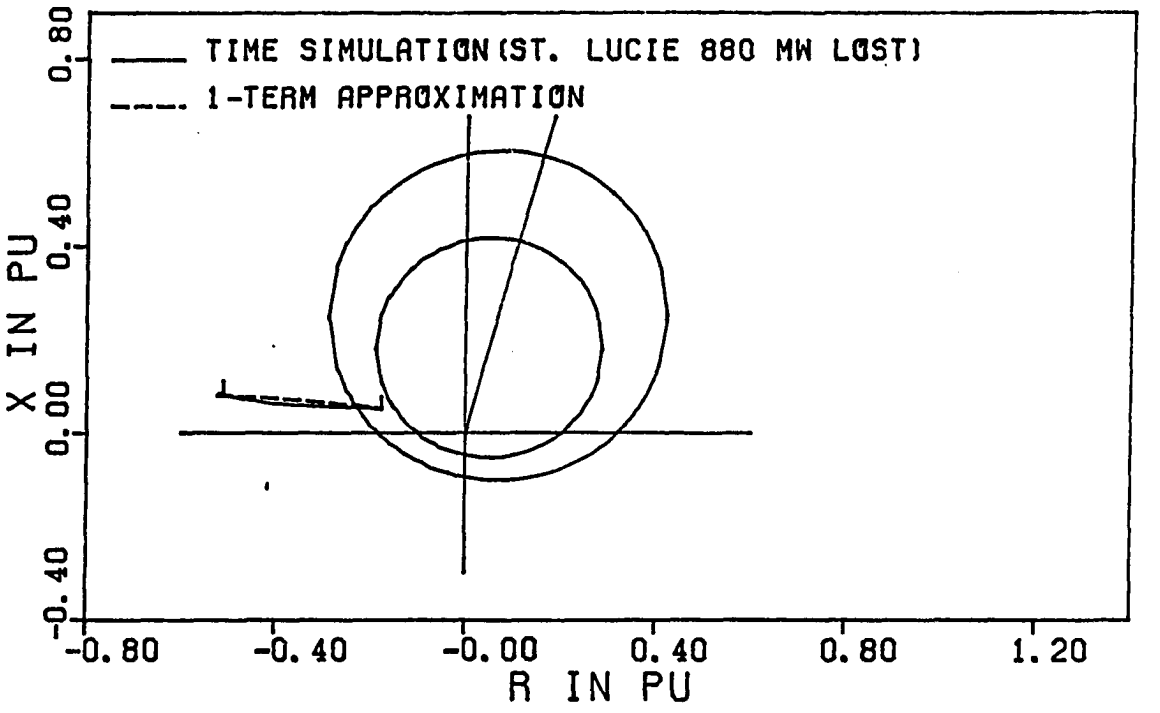

FIGURE 11. Loss of 880 Mw of generation at St. Lucie: 1-term approximation based on the system energy

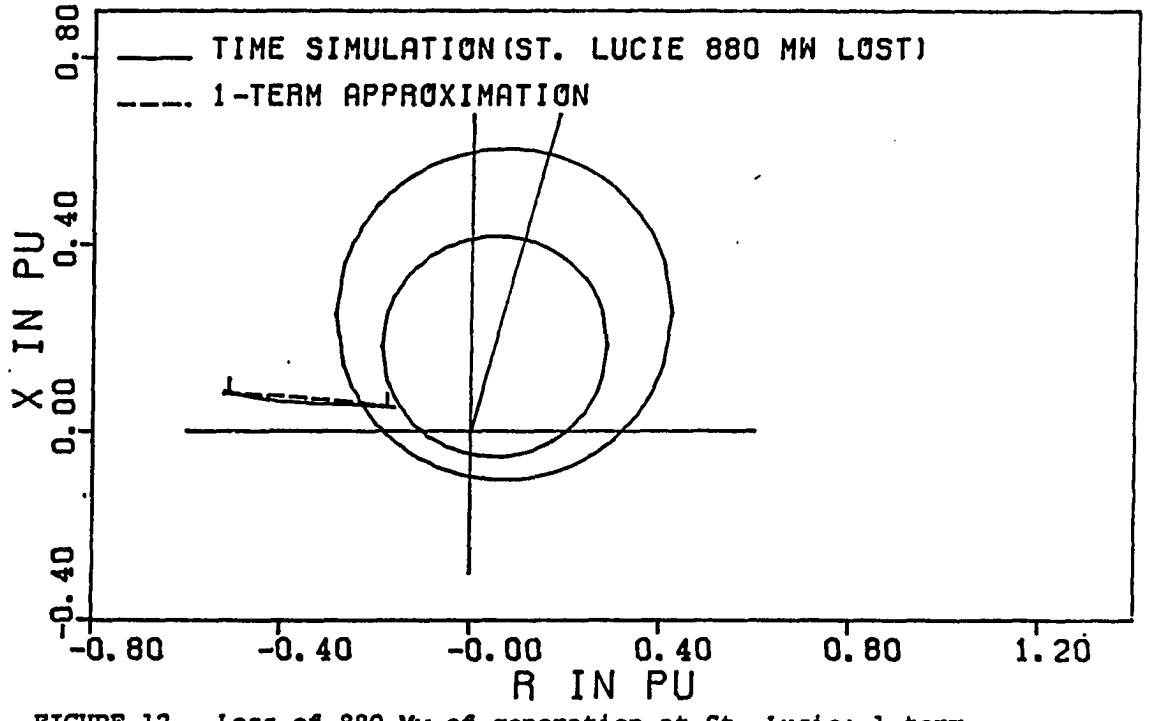

FIGURE 12. Loss of 880 Mw of generation at St. Lucie: 1-term approximation based on the equivalent energy

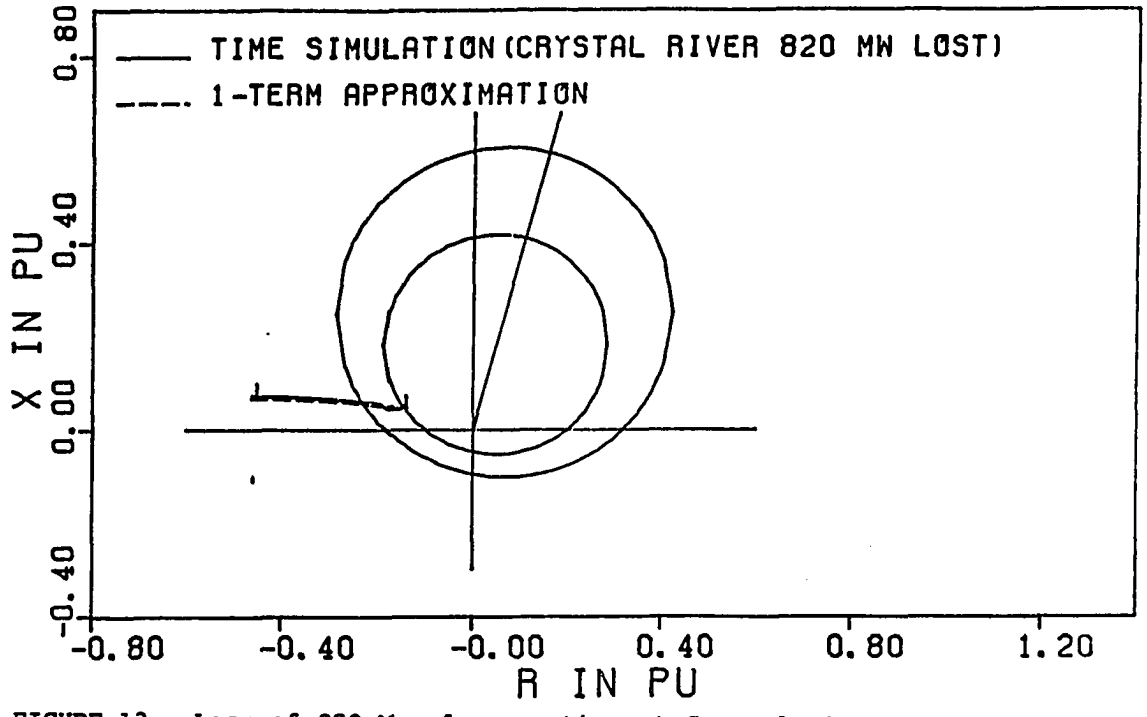

FIGURE 13. Loss of 820 Mw of generation at Crystal River: 1-term approximation based on the system energy

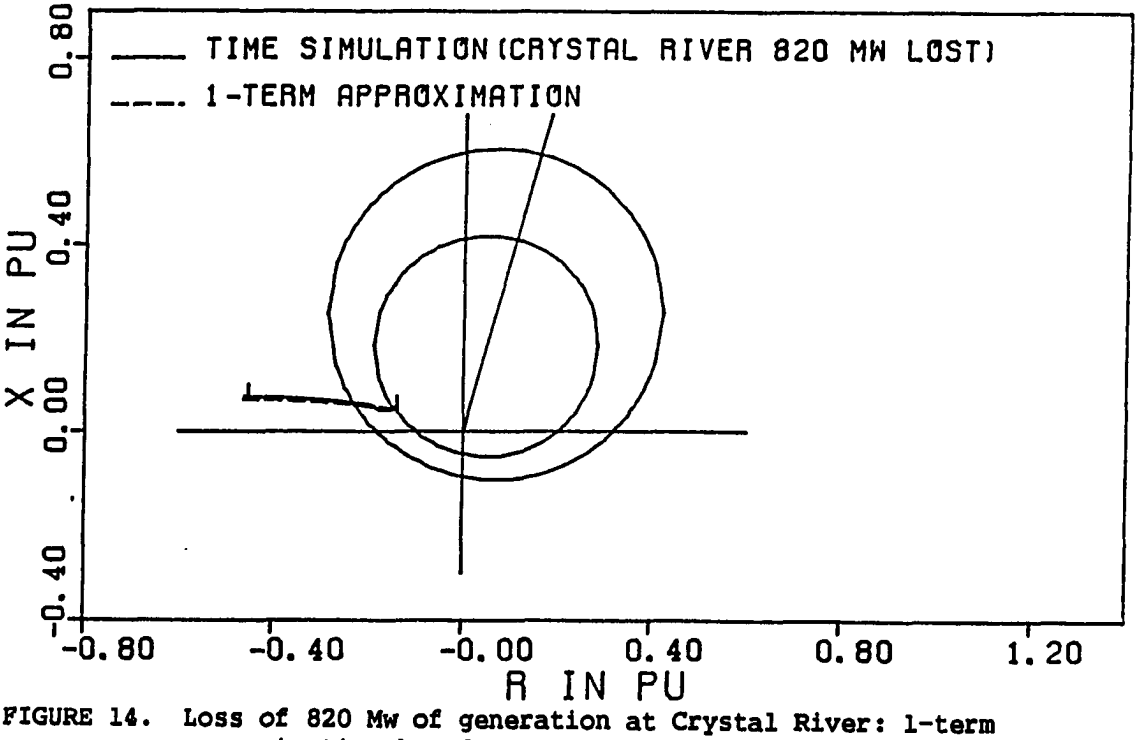

FIGURE 14. Loss of 820 Mw of generation at Crystal River: 1-term approximation based on the equivalent energy

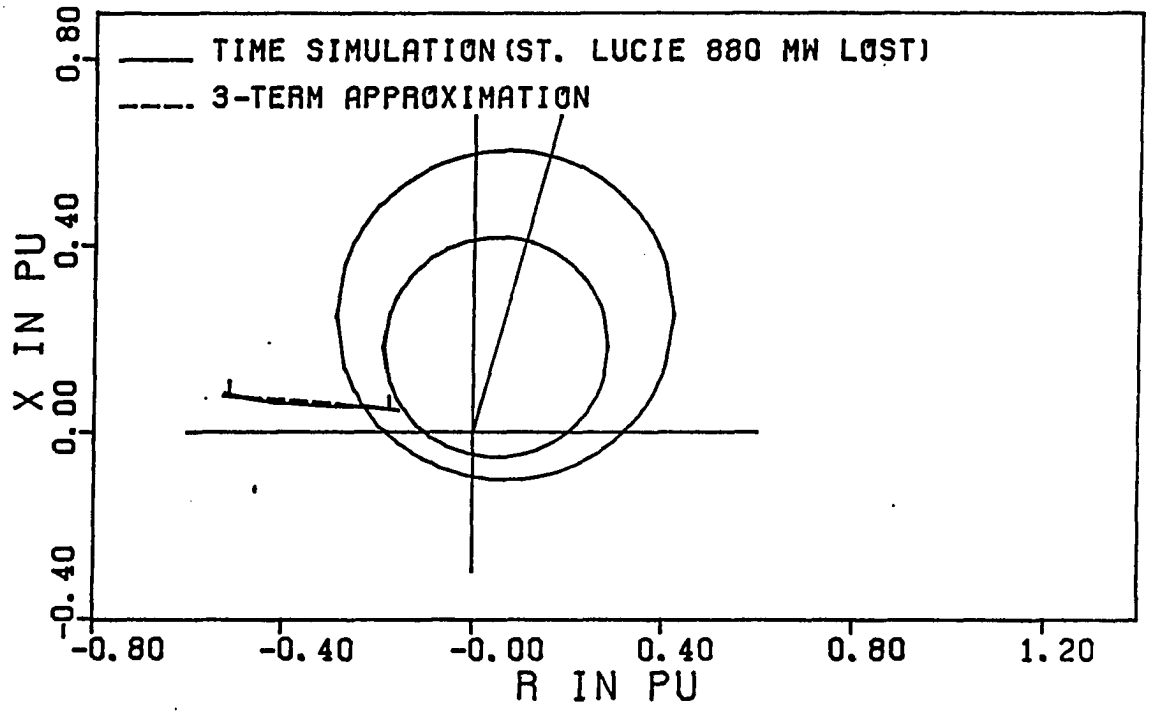

FIGURE 15. Loss of 880 Mw of generation at St. Lucie: 3-term approximation based on the system energy

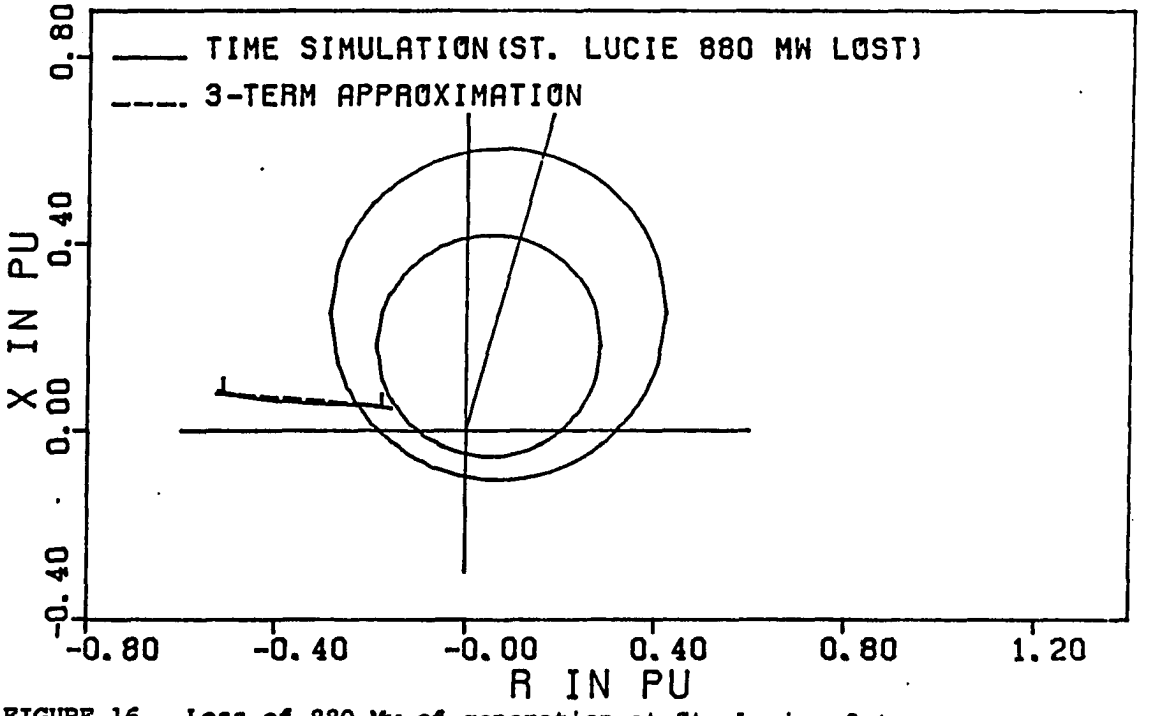

FIGURE 16. Loss of 880 Mw of generation at St. Lucie: 3-term approximation based on the equivalent energy

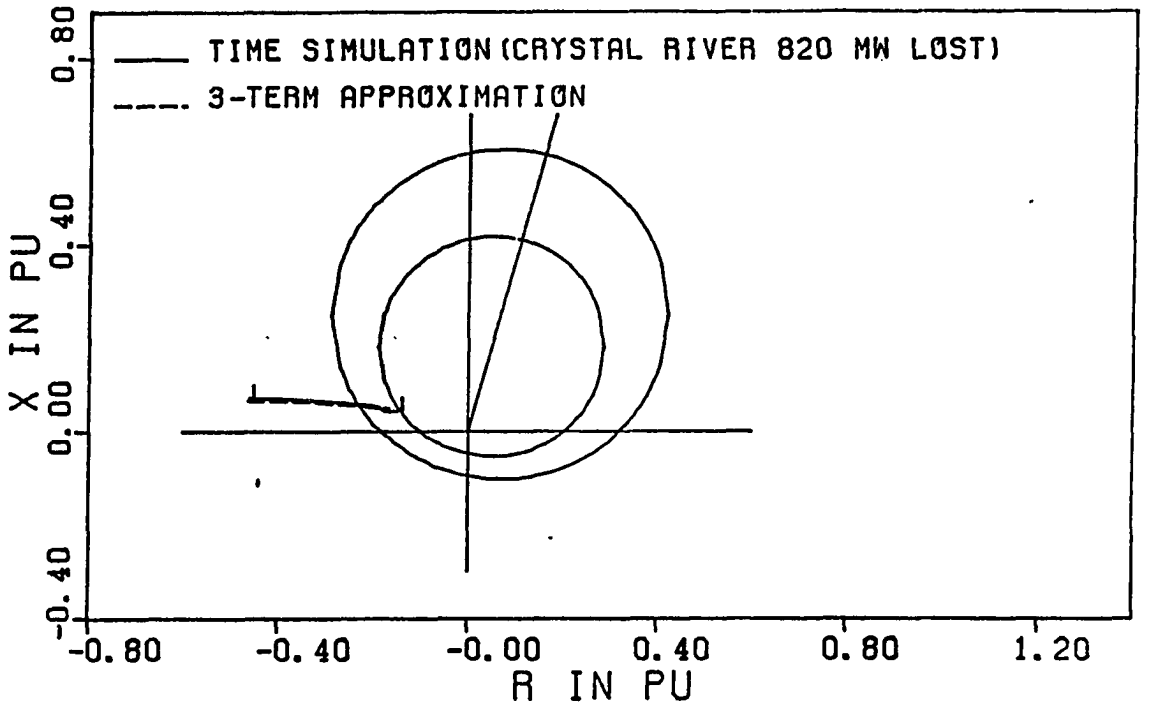

FIGURE 17. Loss of 820 Mw of generation at Crystal River: 3-term approximation based on the system energy

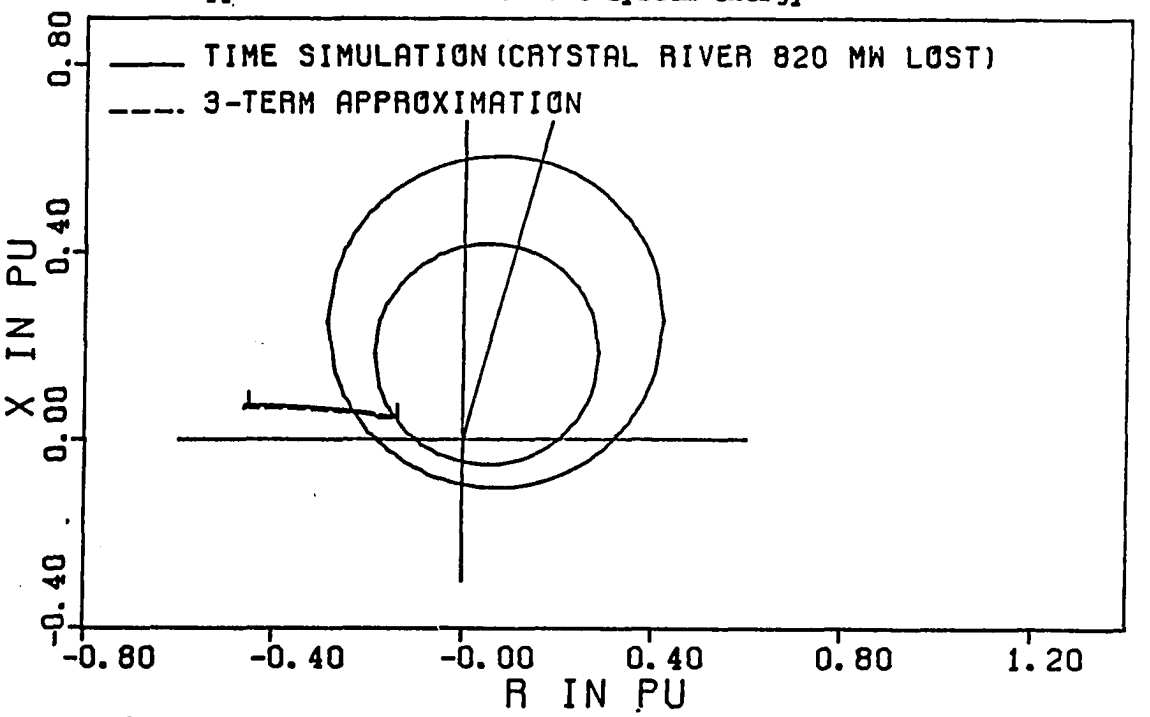

FIGURE 18. Loss of 820 Mw of generation at Crystal River: 3-term approximation based on the equivalent energy

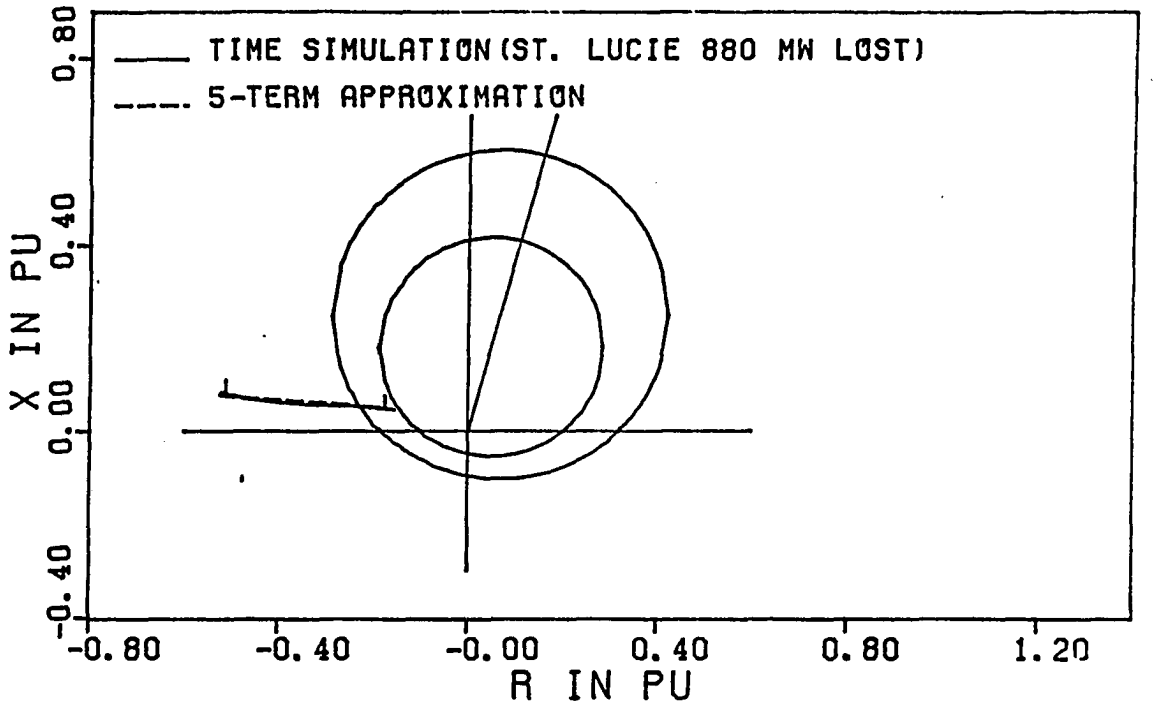

FIGURE 19. Loss of 880 Mw of generation at St. Lucie: 5-term approximation based on the system energy

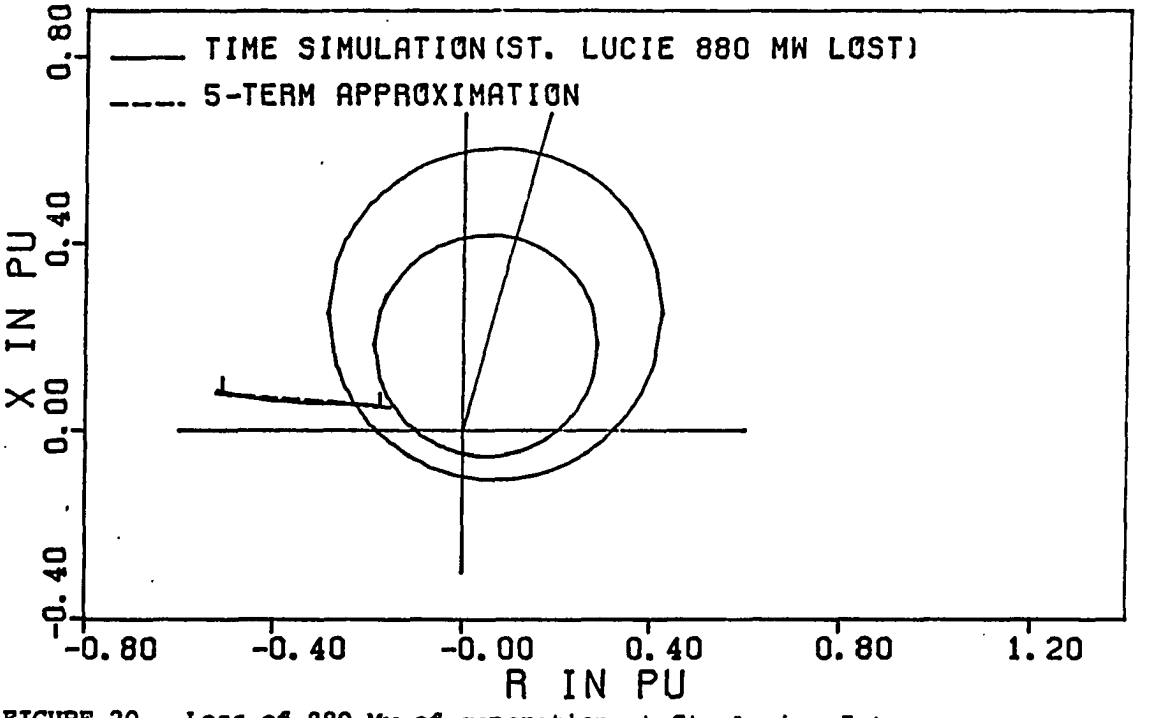

FIGURE 20. Loss of 880 Mw of generation at St. Lucie: 5-term approximation based on the equivalent energy

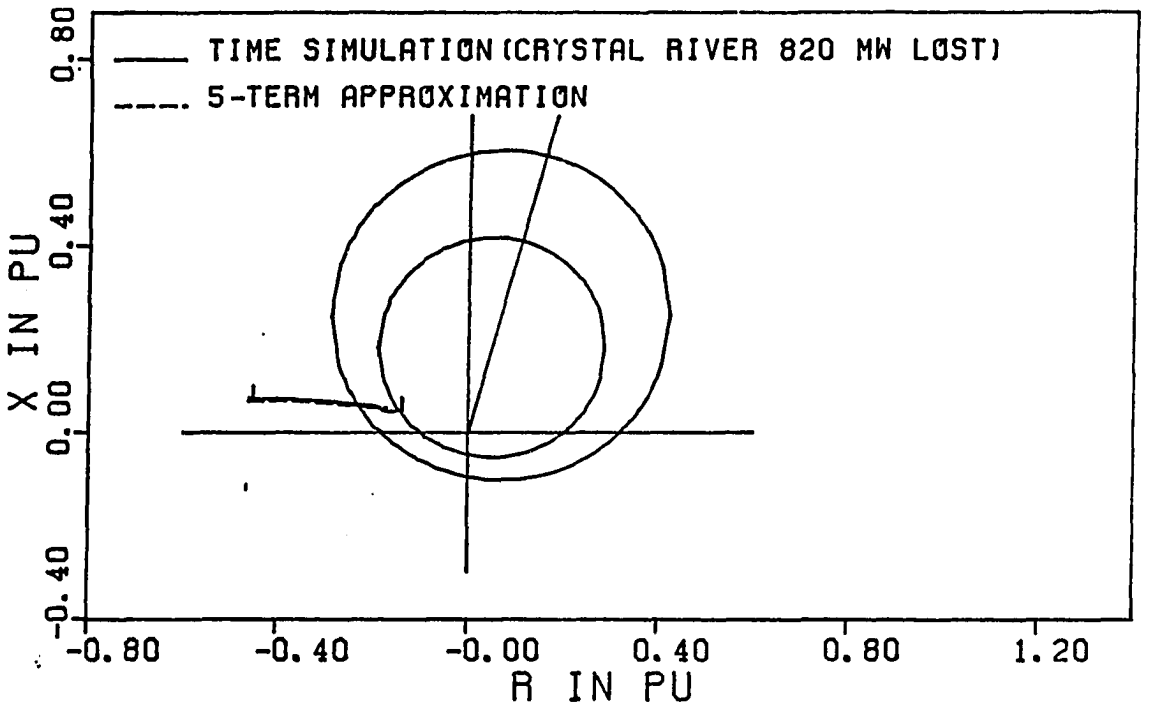

FIGURE 21. Loss of 820 Mw of generation at Crystal River: 5-term approximation based on the system energy

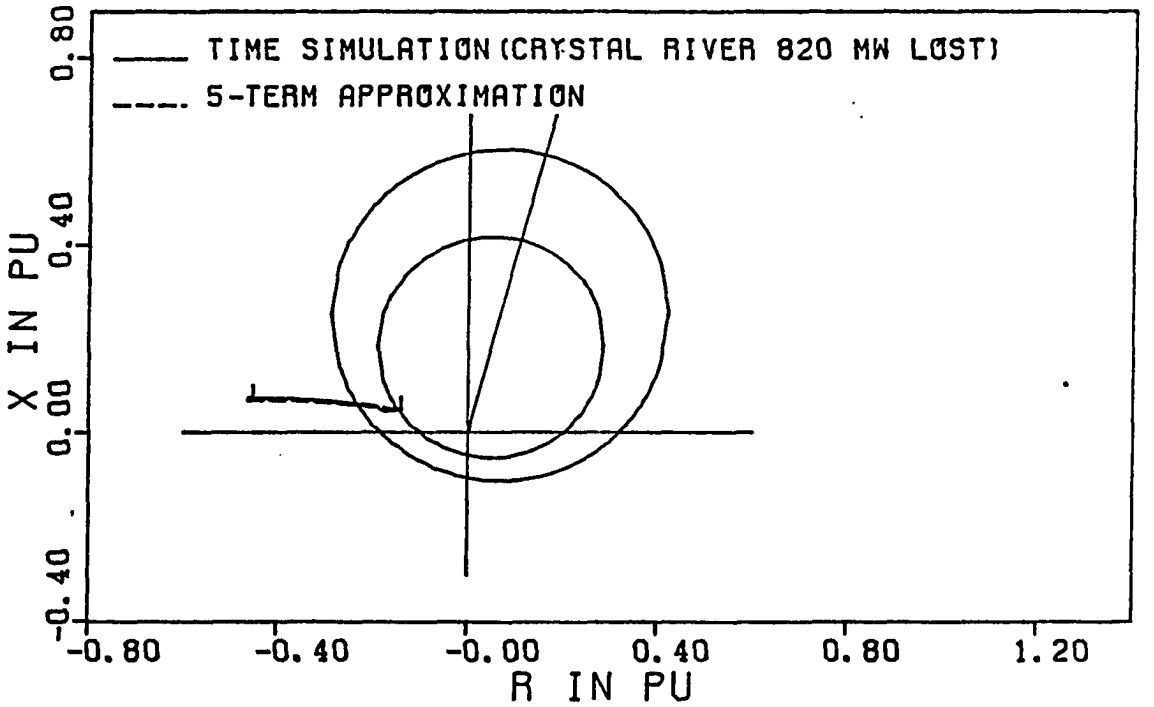

FIGURE 22. Loss of 820 Mw of generation at Crystal River: 5-term approximation based on the equivalent energy

close comparison of the final point on the swing impedance locus.

- While the linear and the 1-term approximations to the trajectory give the similar swing impedance locus, the 3-term and 5-term approximations to the trajectory provide the similar swing impedance locus.
- The 3-term and the 5-term approximations give better results than when the linear or the 1-term approximation is used.

Figures 23-37 show the swing impedance loci for the four other cases obtained by increasing the level of generation lost. The results displayed in Figures 23-37 indicate the followings:

- While the starting points of the swing impedance loci moved away from the relay zone to left as the level of generation lost is increased, the end points of those loci moved inside the relay zone further.
- The patterns of the swing impedance locus do not change as the level of generation lost is increased.
- In all the cases analyzed, the maximum error between the minimum apparent impedances obtained by the approximations and that obtained by time simulation is 2.58 %.

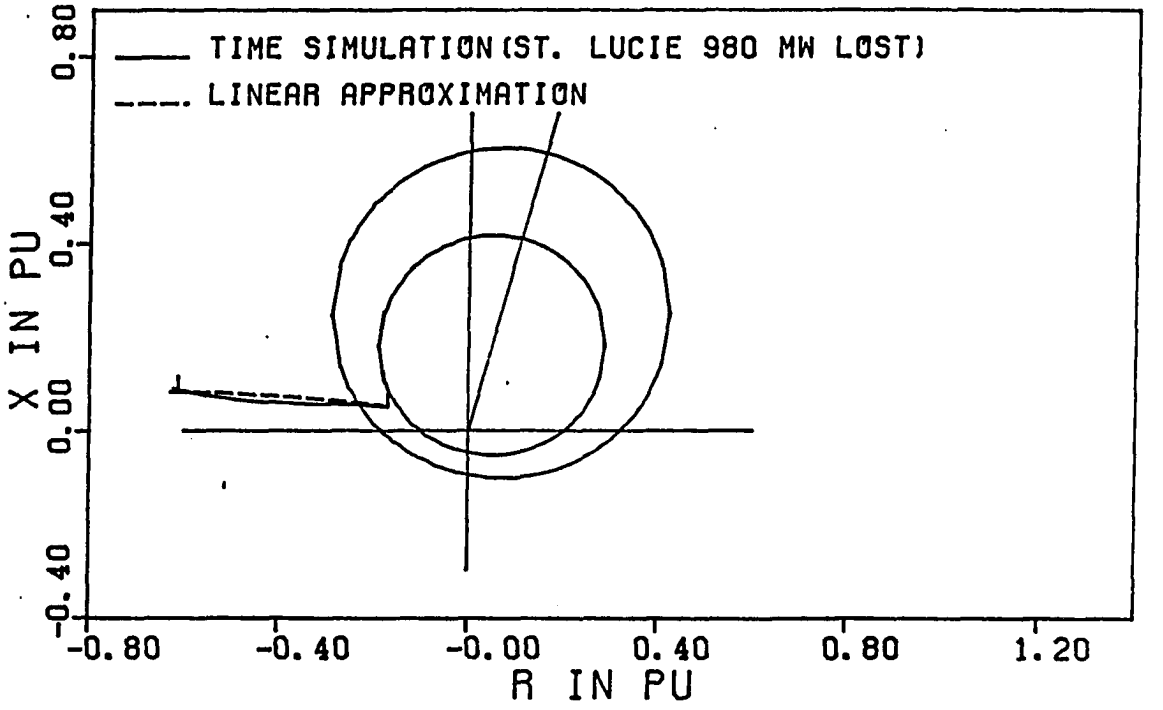

FIGURE 23. Loss of 980 Mw of generation at St. Lucie: linear approximation based on the system energy

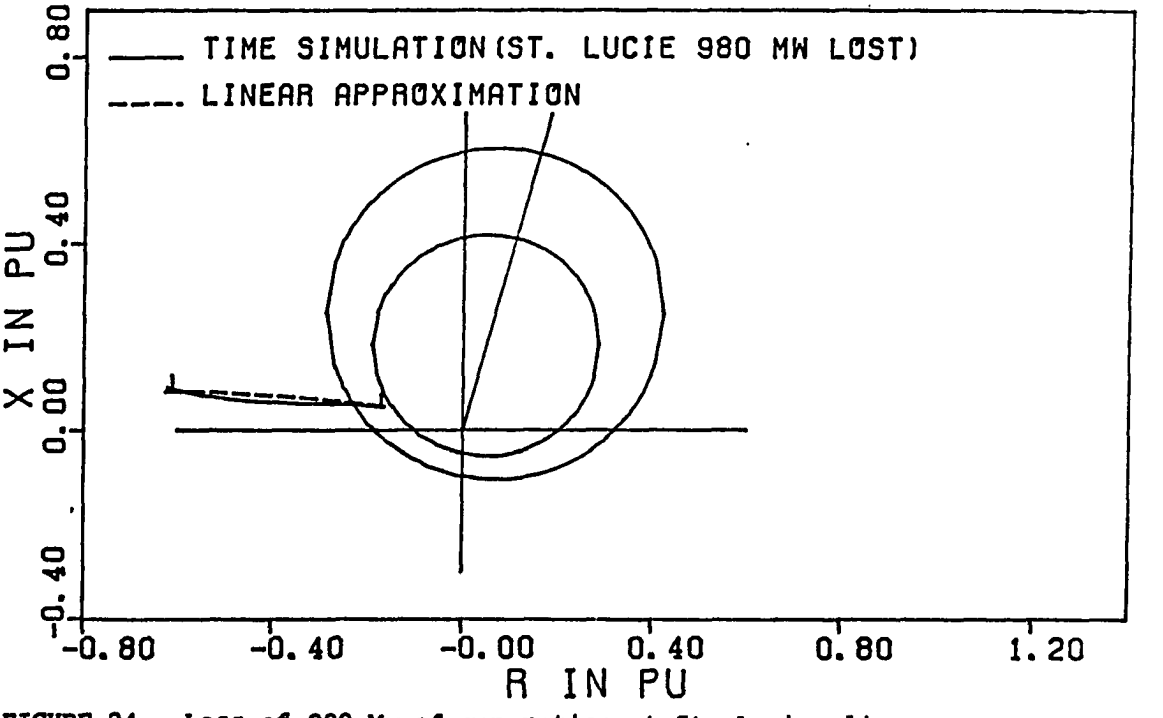

FIGURE 24. Loss of 980 Mw of generation at St. Lucie: linear approximation based on the equivalent energy

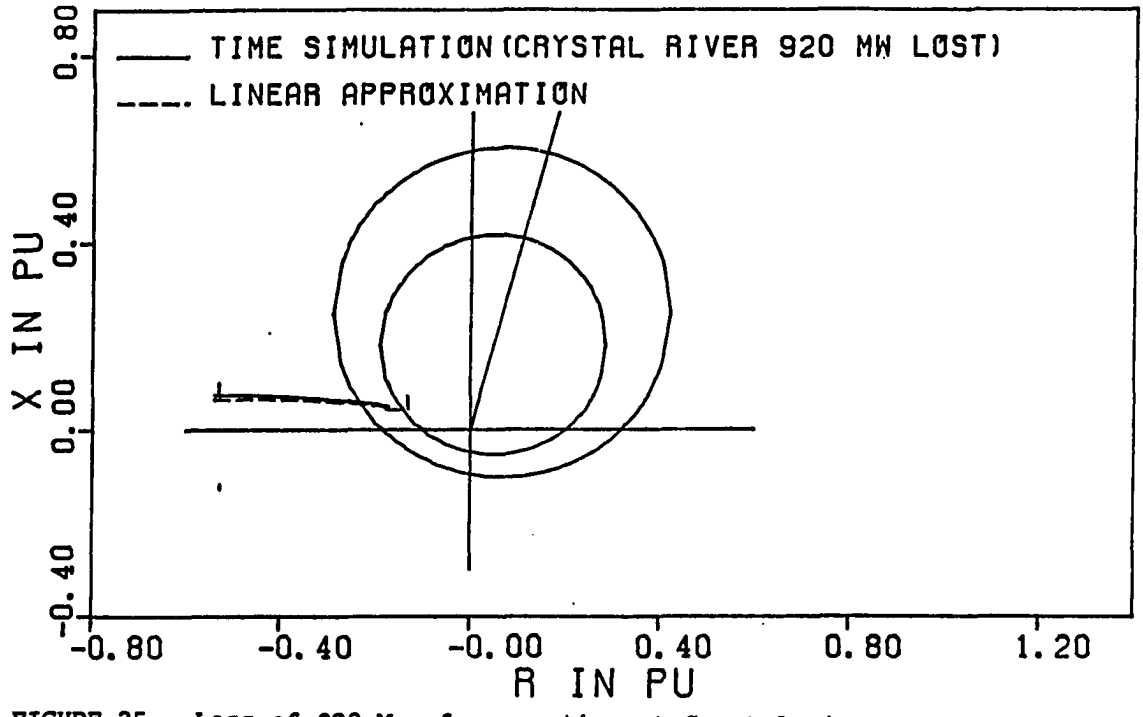

FIGURE 25. Loss of 920 Mw of generation at Crystal River: linear approximation based on the system energy

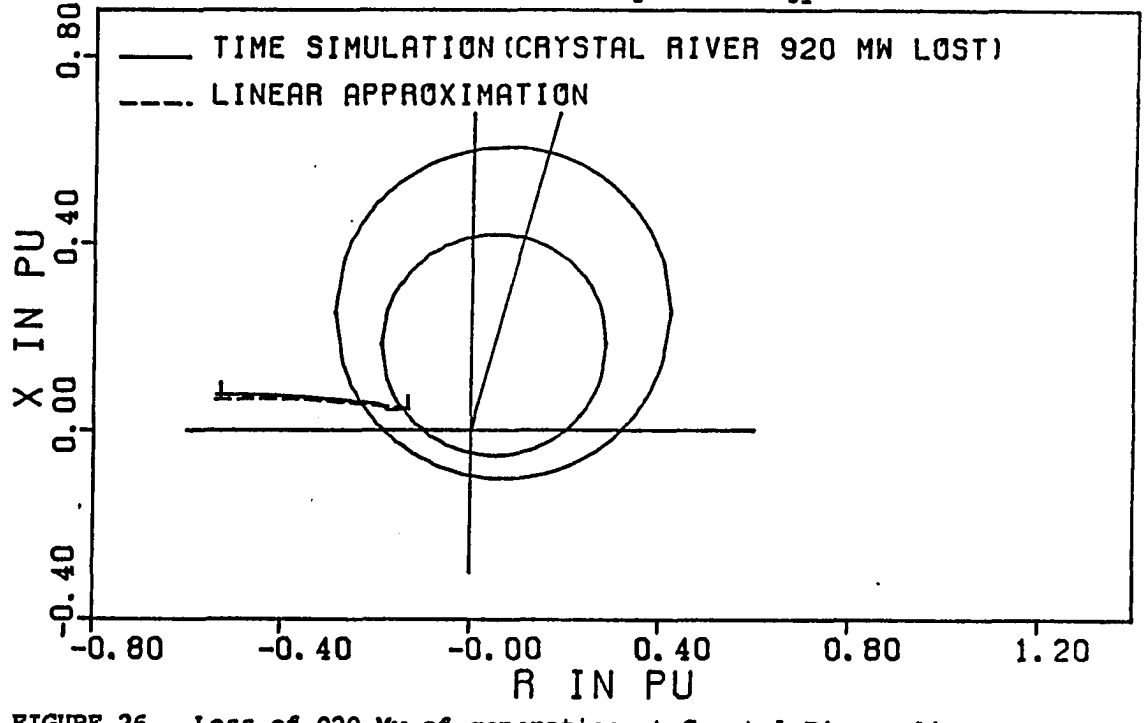

FIGURE 26. Loss of 920 Mw of generation at Crystal River: linear approximation based on the equivalent energy

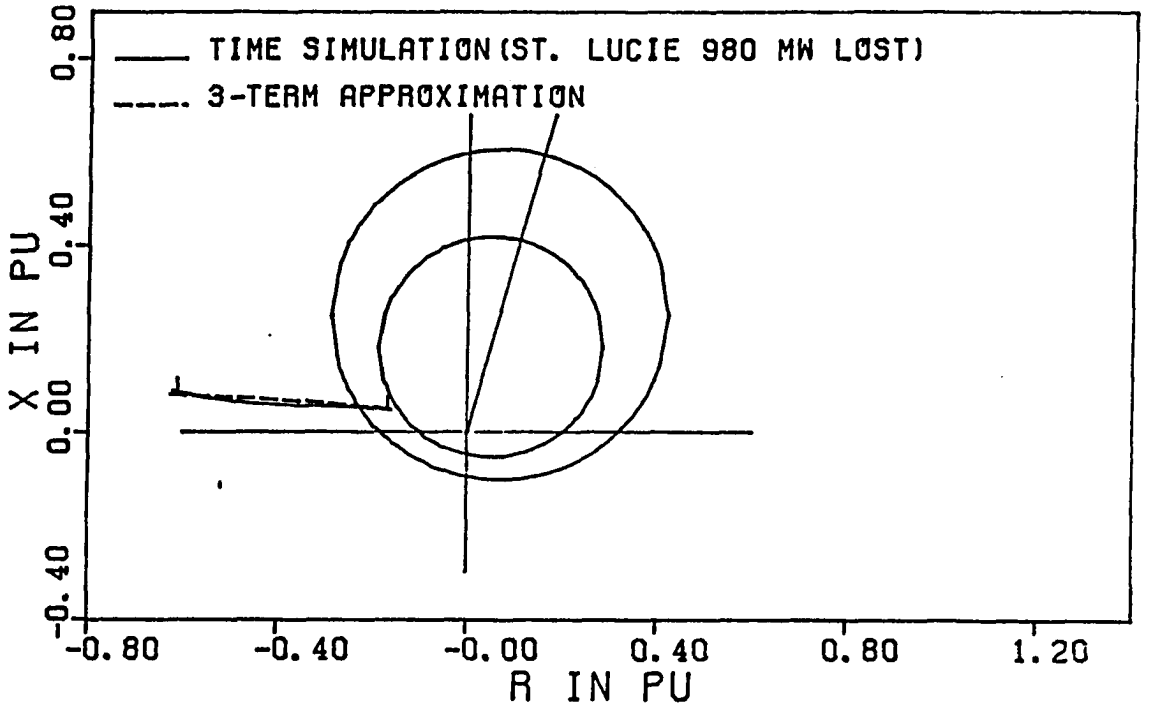

FIGURE 27. Loss of 980 Mw of generation at St. Lucie: 3-term approximation based on the system energy

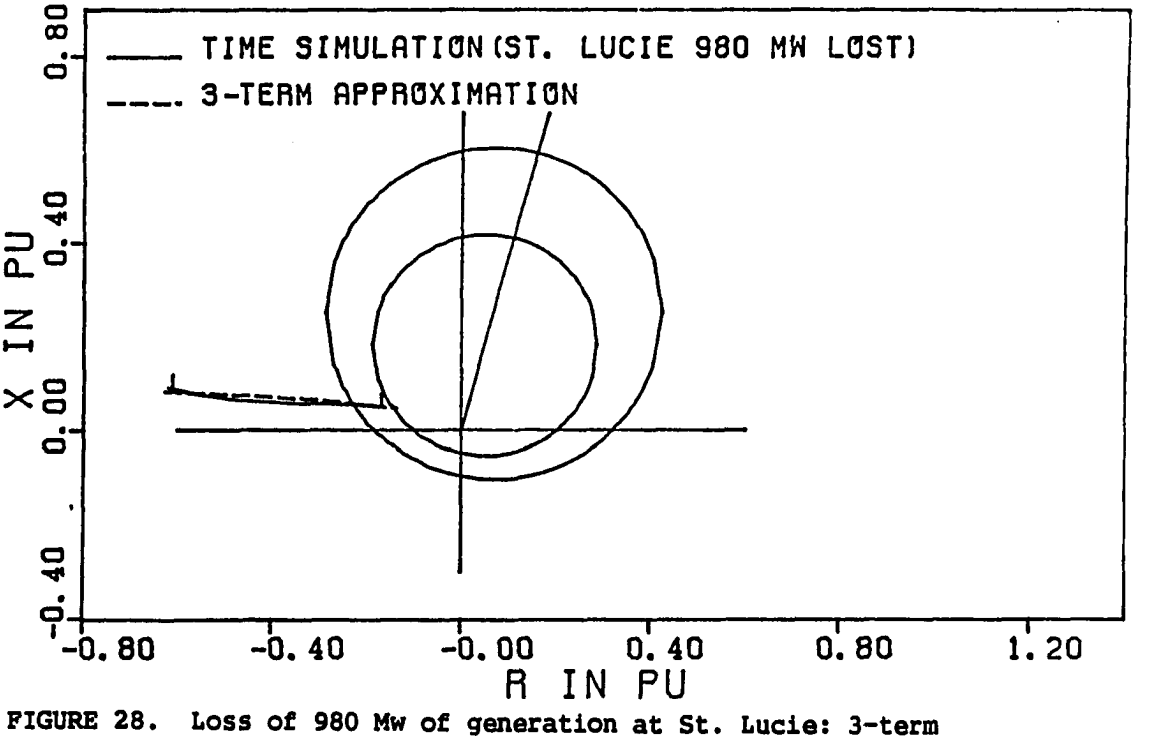

FIGURE 28. Loss of 980 Mw of generation at St. Lucie: 3-term approximation based on the equivalent energy

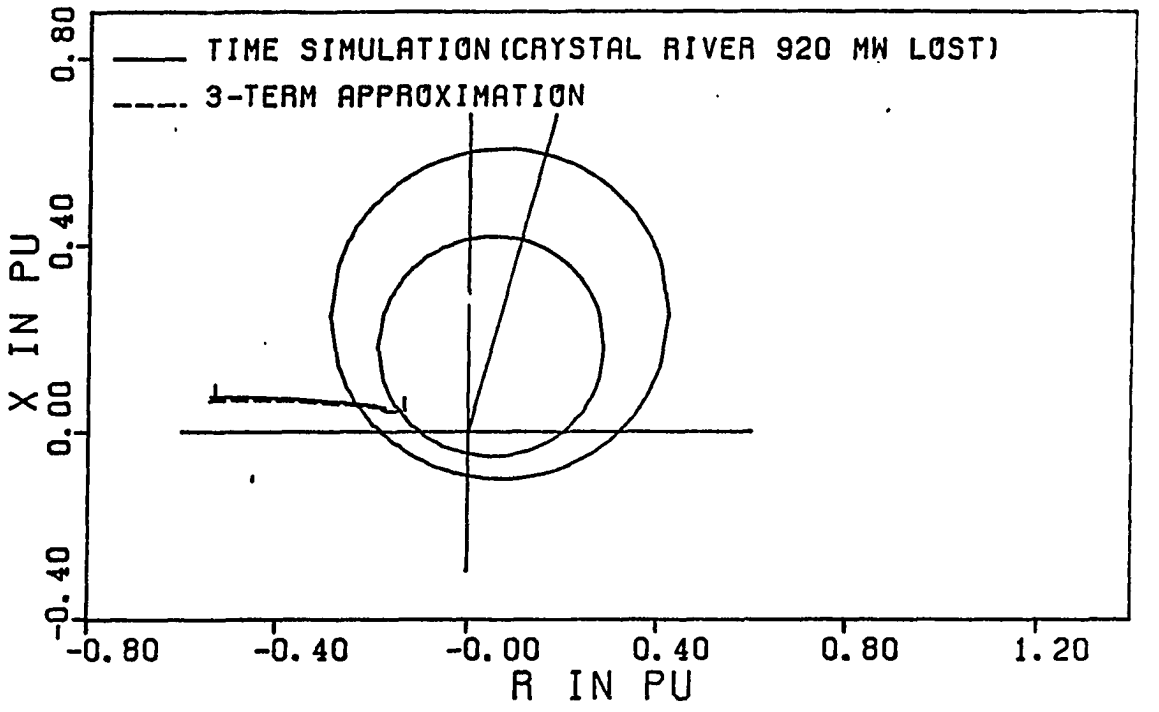

FIGURE 29. Loss of 920 Mw of generation at Crystal River: 3-term approximation based on the system energy

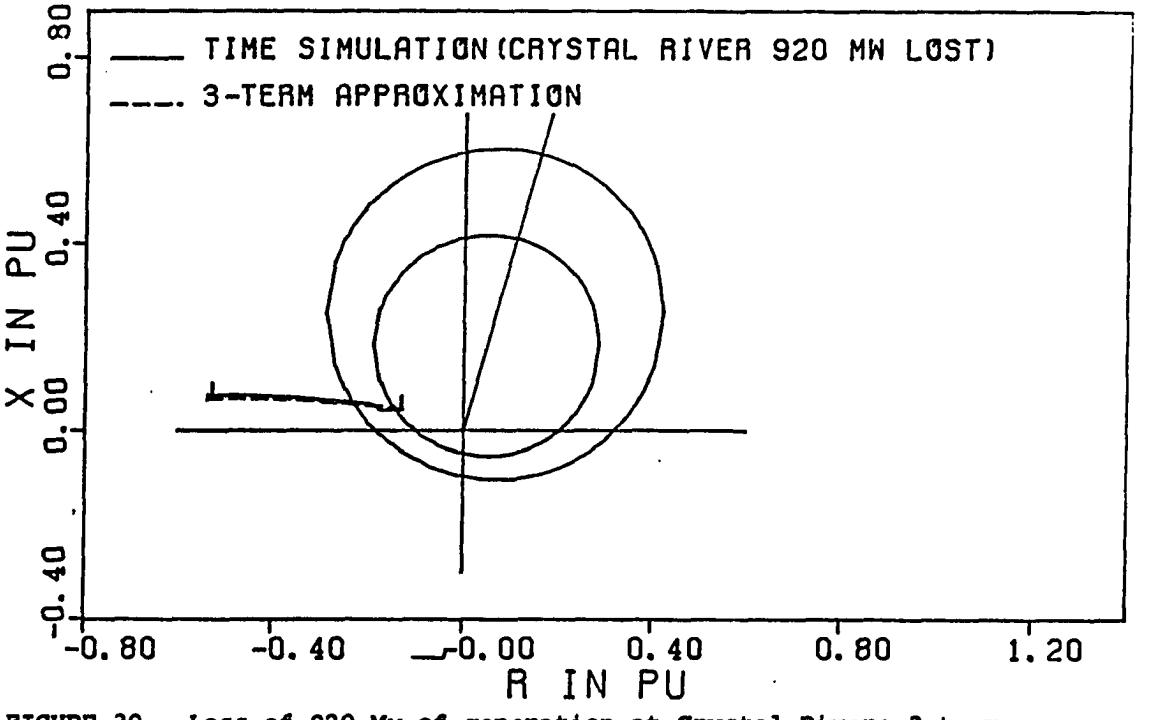

FIGURE 30. Loss of 920 Mw of generation at Crystal River: 3-term approximation based on the equivalent energy

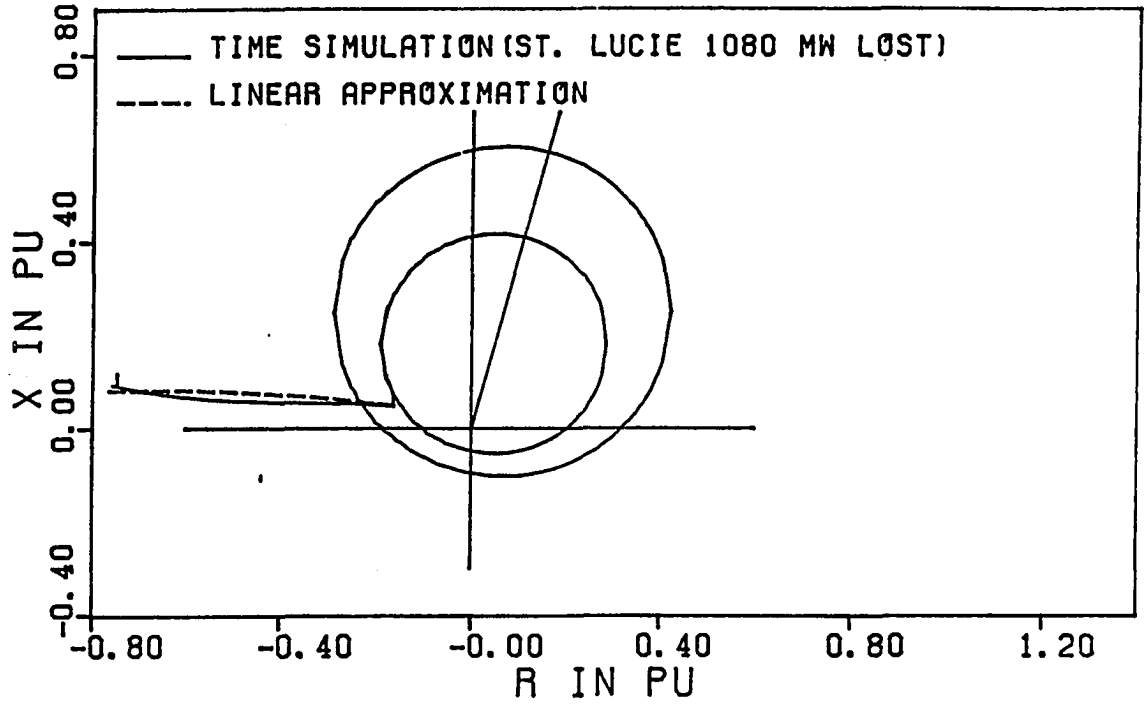

FIGURE 31. Loss of 1080 Mw of generation at St. Lucie: linear approximation based on the system energy

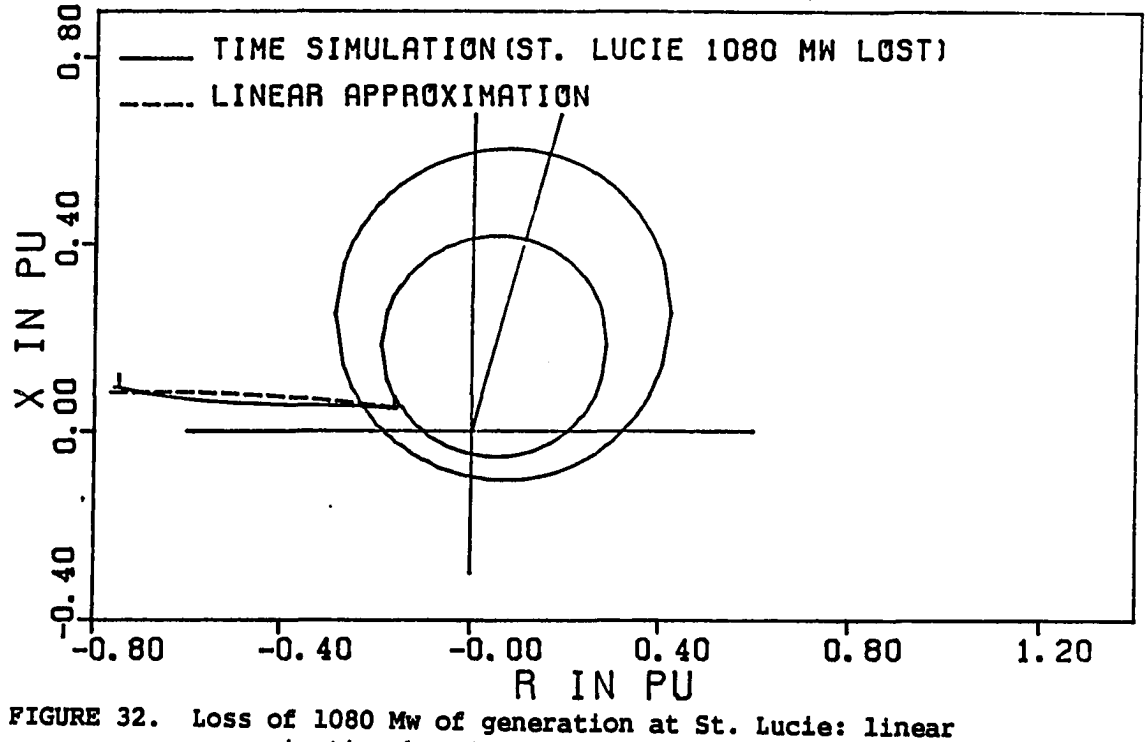

FIGURE 32. Loss of 1080 Mw of generation at St. Lucie: linear approximation based on the equivalent energy

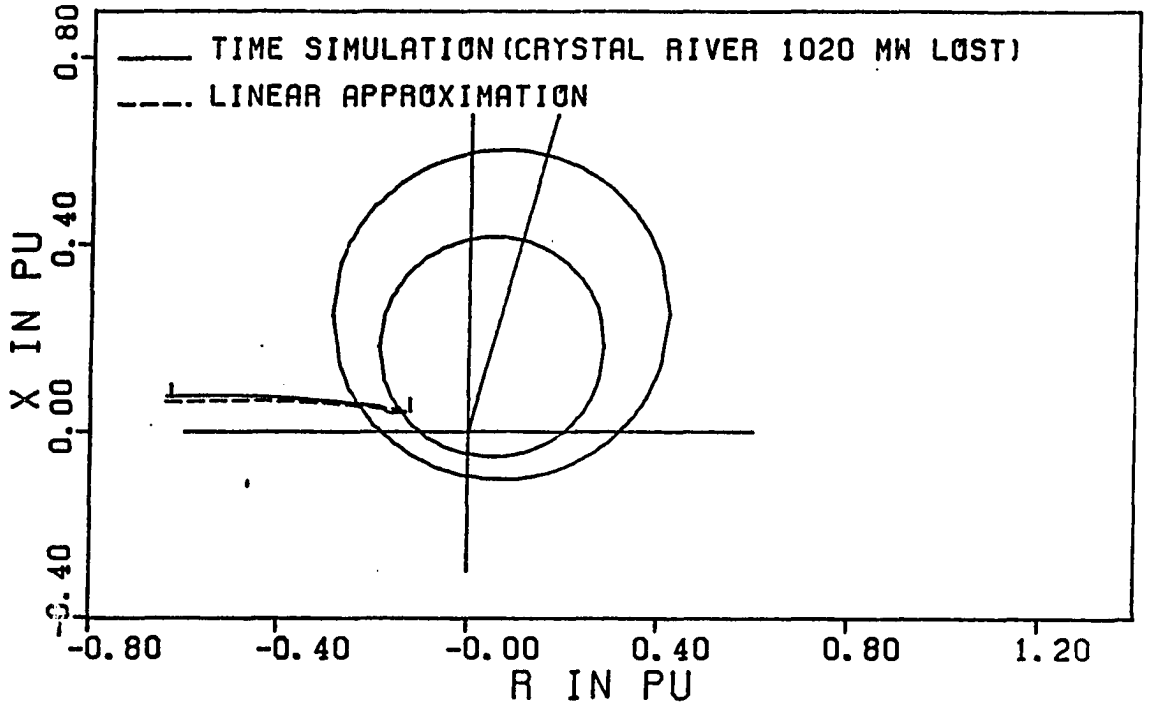

FIGURE 33. Loss of 1020 Mw of generation at Crystal River: linear approximation based on the system energy

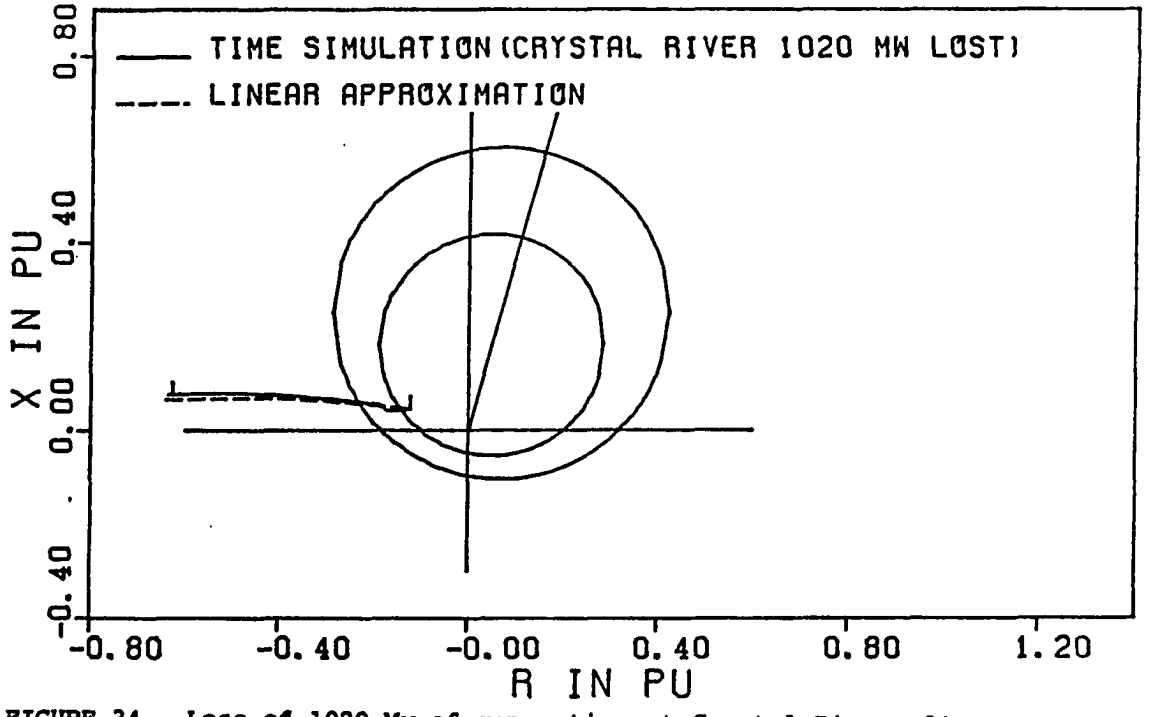

FIGURE 34. Loss of 1020 Mw of generation at Crystal River: linear approximation based on the equivalent energy

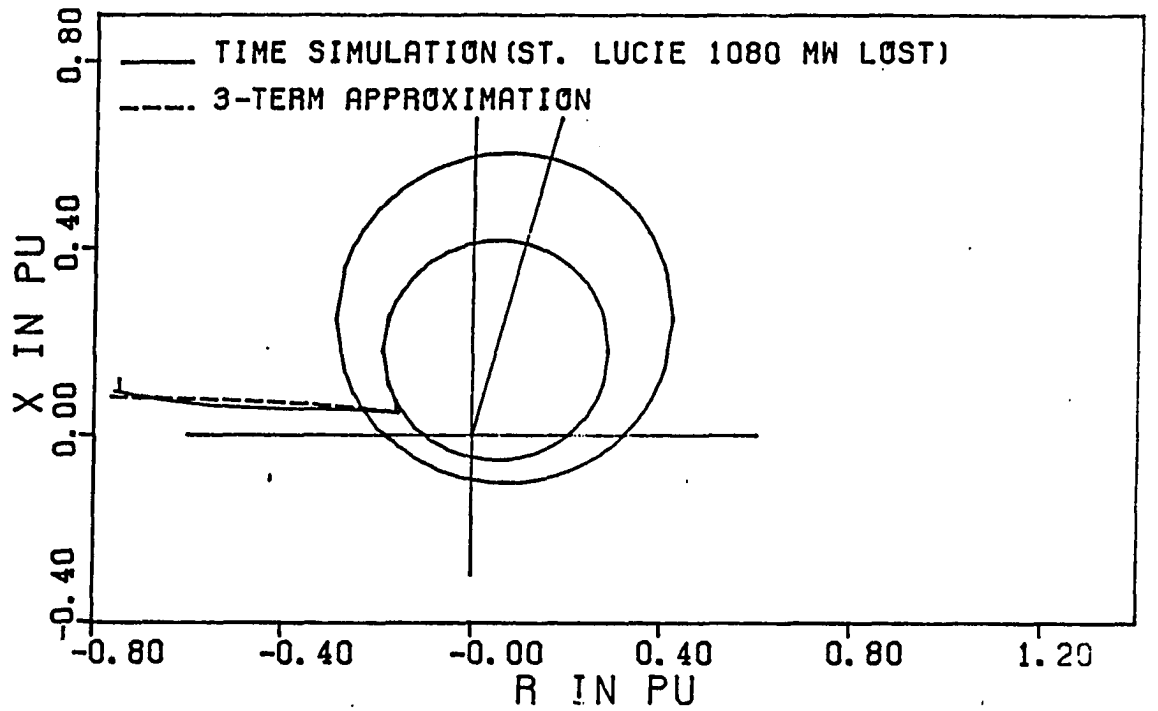

FIGURE 35. Loss of 1080 Mw of generation at St. Lucie: 3-term approximation based on the system energy

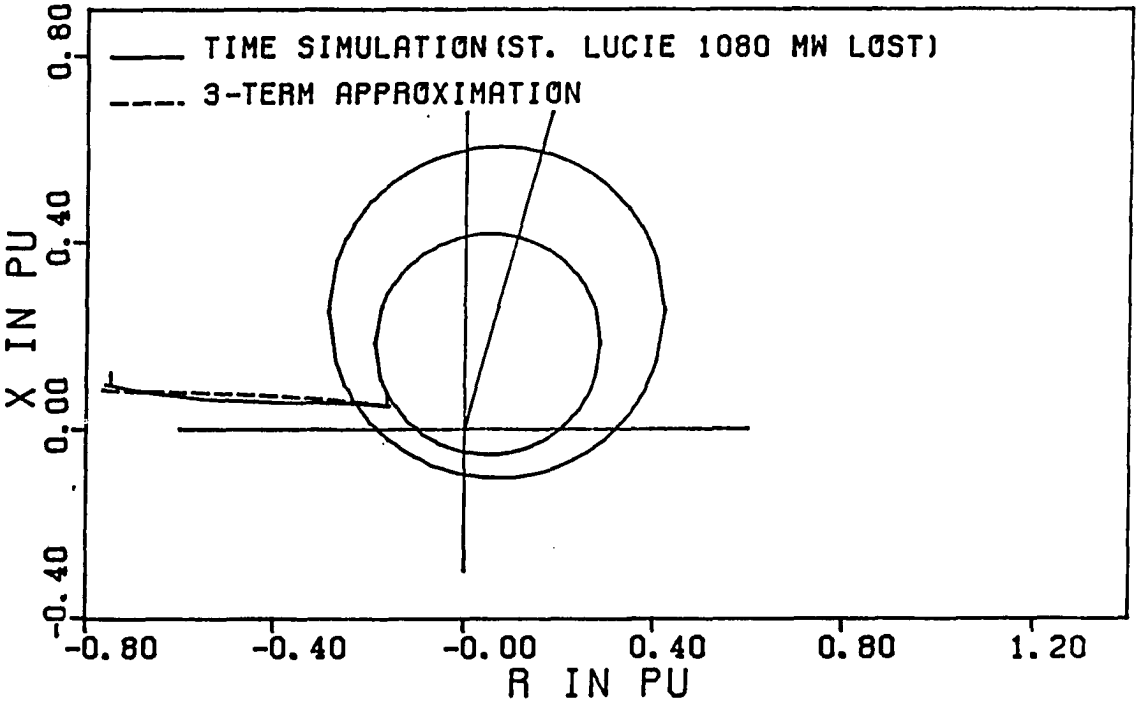

FIGURE 36. Loss of 1080 Mw of generation at St. Lucie: 3-term approximation based on the equivalent energy

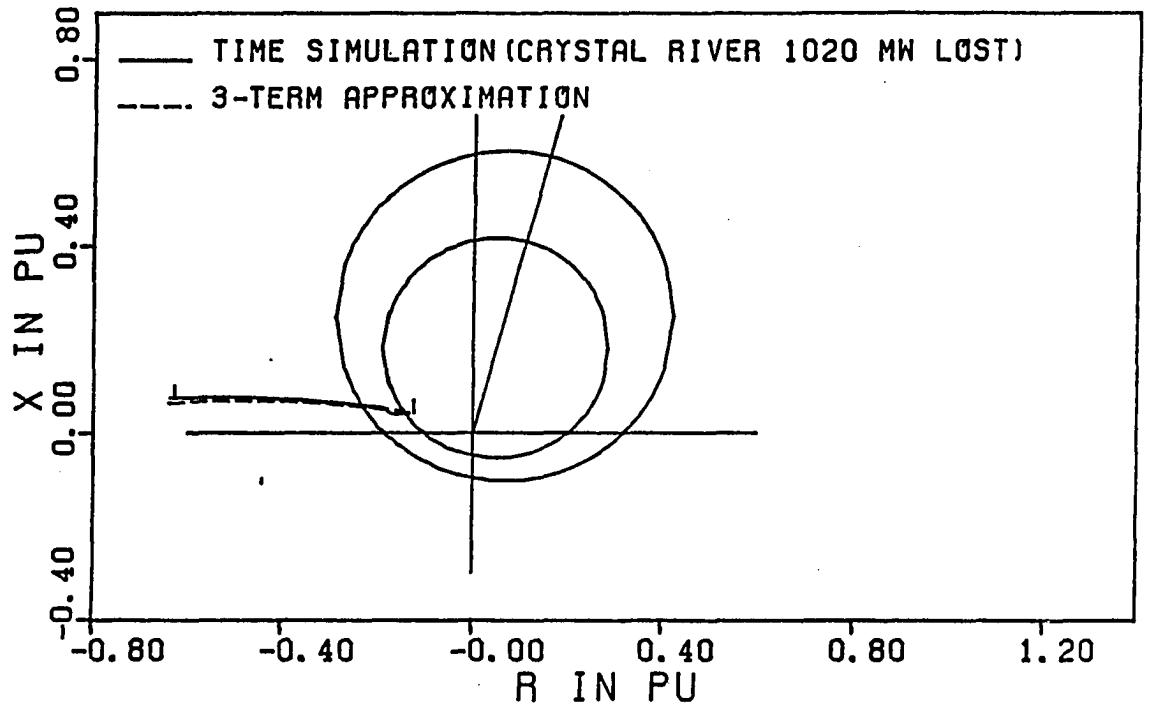

FIGURE 37. Loss of 1020 Mw of generation at Crystal River: 3-term approximation based on the system energy

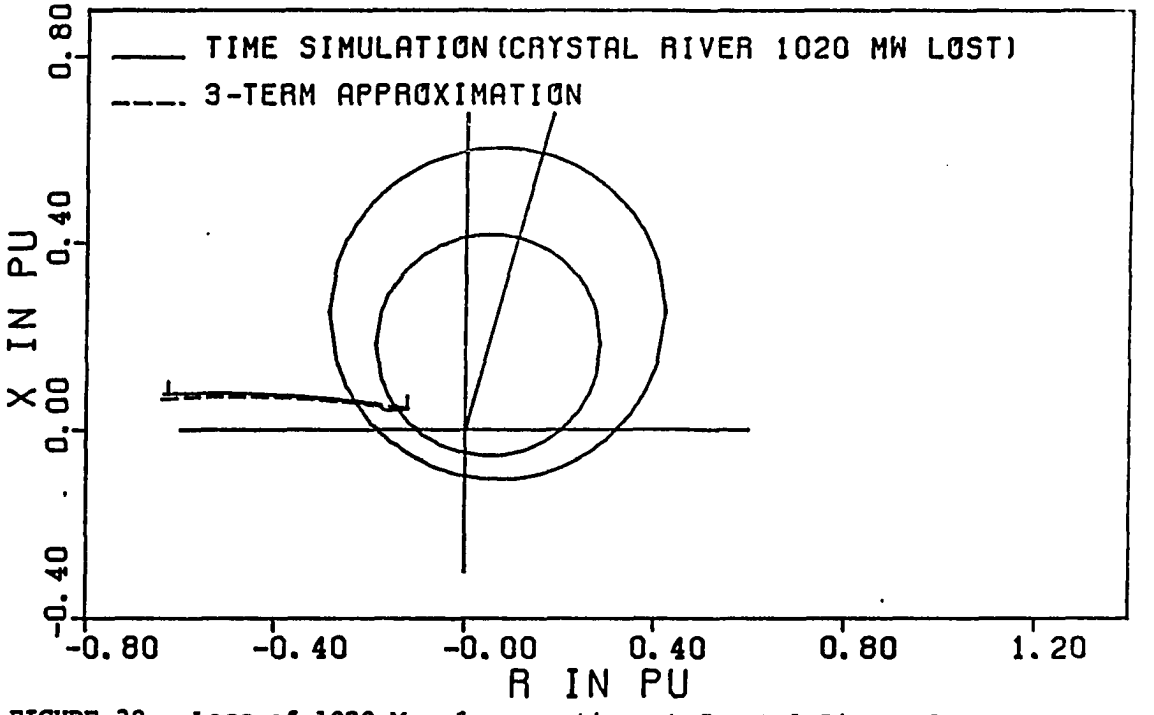

FIGURE 38. Loss of 1020 Mw of generation at Crystal River: 3-term approximation based on the equivalent energy

CHAPTER VII. CONCLUSION

In this dissertation, a procedure was presented in which the transient energy margin, obtained by the transient energy function method, was used to detect if the zone of the out-of-step relays is entered during the first swing transient following a particular disturbance. The procedure was validated by comparing minimum apparent impedance seen by out-of-step relay and the swing impedance locus obtained from the proposed procedure with those obtained from time simulation.

The dissertation suggests that a two machine equivalent formulated at the fictitious inertial centers of two groups of machines provides a better explanation of the effects of the swings of the synchronous machines on the apparent impedance "seen" by the out-of-step relays. The information to obtain such a two machine equivalent is provided by the controlling u.e.p.: i) the grouping of the critical machines indicated by rotor angles greater than + 90 degrees or less than - 90 degrees, and ii) the grouping of the rest of the system.

The following conclusions can be drawn from the results presented in this dissertation:

- A technique has been developed to relate the transient energy margin, obtained by the transient energy function method, to the point of minimum apparent impedance on a line protected by the out-of-step relay. The energy margin based on both the total system energy and the two machine equivalent energy give minimum apparent impedances which compare well with those obtained from time simulation.

- A procedure to obtain the swing impedance locus using an approximation to the system trajectory is proposed.
- A technique to obtain an approximation to the post-disturbance trajectory is proposed. The proposed technique utilizes the information at two points: i) at the instant of disturbance removal, and ii) the controlling u.e.p.

  Two types of approximation are proposed: i) the linear trajectory approximation, and ii) the series approximation using the first few terms of the Fourier series.
- The technique is tested for loss of generation disturbances in an equivalent of the Florida Power & Light company network. The technique accurately predicts the point of minimum apparent impedance and satisfactorily provides the swing impedance locus.
- This procedure represents the first attempt to relate the transient energy margin obtained by the transient energy function method from a reduced formulation of a power system to some parameter within the network. This concept could be extented to other parameters which need to be monitored.
- The procedure can be incorporated into rapid transient stability assessment by the transient energy function method in order to obtain the voltage profile at some important load buses.
- The research presented in this dissertation extends the applicability of the transient energy function method to power systems.

  1). It may help in offering guidelines for setting out-of-step

relays.

2). It overcomes some of the current limitations of the transient energy function method [48] about not providing information within the network.

Suggestion for Future Research

On the basis of the investigation conducted in this research work, some of the problems that need further attention are:

- Implementing aspects of the out-of-step relay reported in [39,40] into the transient energy function method. This subject is of particular interest because the rate of change of the apparent impedance seen by out-of-step relay can be described as a function of the generators' rotor angles and velocities.
- Implementing a procedure that will monitor voltage at some key buses in the network following a disturbance. This dissertation suggested a formulation that will provide the voltage profile at some load buses. The formulation in the dissertation was used to obtain the swing impedance locus. The development of a procedure that will provide the voltage profile at some key buses and compare them to those obtained from time simulation through a parameter variable such as potential energy may extend the applicability of the transient energy function method further.

BIBLIOGRAPHY

1. IEEE Committee Report. "Proposed Terms and Definitions For Power System Stability." IEEE Trans., PAS-101 (1982): 1894-1898.

2. Proceedings of the International Symposium on Power System Stability, Ames, Iowa: Iowa State University Press, 1985.

3. Kimbark, E. W. Power System Stability. Vol. I. New York: John Wiley & Sons, Inc., 1948.

4. Crary, S. B. Power System Stability. Vol. II. New York: John Wiley & Sons, Inc., 1948.

5. Criteria of Stability of Electric Power Systems. A Report. Union Institute of Scientific and Technological Information and the Academy of Sciences of the U.S.S.R Electric Power Series, Moscow, 1971.

6. Magnuson, P. C. "Transient Energy Method of Calculating Stability." AIEE Trans., PAS-66 (1947): 745-755.

7. Aylett, P. D. "The Energy Integral Criterion of Transient Stability Limits of Power Systems." Proceedings of IEEE 105 (C) (1958): 527-536.

8. Gless, G. E. "Direct Method of Lyapunov Applied to Transient Power Stability." IEEE Trans., PAS-85 (Feb. 1966): 158-168.

9. El-Abiad, A. H. and Nagappan, K. "Transient Stability Regions of Multimachine Power Systems." IEEE Trans., PAS-85 (Feb. 1966): 169-179.

10. Miller, R. K. and Michel, A. N. Ordinary Differential Equations. New York: Academia Press, 1982.

11. Vidyasagar, M. Nonlinear Systems Analysis. Eaglewood Cliff, New Jersey: Prentice-Hall, 1978.

12. Pai, M. Power System Stability by the Direct Method of Lyapunov. North-Holland Systems and Control Series Vol. III. New York: North-Holland Publishing Company, 1981.

13. Fouad, A. A. "Stability Theory: Criteria for Transient Stability." Proceedings of Conference on Systems Engineering for Power: Status and Prospects. Huniker, N.H., 1975.

14. Ribbens-Pavella, M. "Critical Survey of Transient Stability Studies of Multimachine Power Systems by Lyapunov's Direct Method." Proceedings of 9th Annual Allerton Conference on Circuits and Systems Theory. Oct., 1971.

15. Fouad, A. A., Kruempel, K. C., Mamandur, K. R. C., Stanton, S. E, Pai, M. A., and Vittal, V. "Transient Stability Margin as a Tool for Dynamic Security Assessment." EPRI Report EL-1755, March 1981.

16. Tavora, C. J. and Smith, O. J. M. "Characterization of Equilibrium and Stability in Power Systems." IEEE Trans., PAS-91 (May/June 1972): 1127-1145.

17. Lugtu, R. L. and Fouad, A. A. "Transient stability analysis of Power Systems Using Lyapunov's Second methods." IEEE Conference paper No.C72145-6.

18. Athay, T., Sherkat, V. R., Podmore, R., Virmani, S., and Puech, C. "Transient Energy analysis." Systems Engineering for Power: Emergency operating State Control. U.S. Department of Energy. Publication No. CONF-790904-IL.

19. Athay, T., Podmore, R. and Virmani, S. "A Practical Method for Direct Analysis of Transient Stability." IEEE Trans., PAS-98 No.2 (1979): 573-584.

20. Fouad, A. A. and Stanton, S. E. "Transient Stability of a Multimachine Power System. PART I: Investigation of the System Trajectory. PART II: Critical Transient Energy." IEEE Trans., PAS-100 (1981): 3408-3424.

21. Prabhakara, F. S. and El-Abiad, A. H. "A Simplified Determination of Transient Stability Regions for Lyapunov's Methods." IEEE Trans., PAS-94 (March/April 1975): 672-689.

22. Gupta, C. L. and El-Abiad, A. H. "Determination of the Closest Unstable Equilibrium State for Lyapunov's Methods in Transient Stability Studies." IEEE Trans., PAS-95 (September/October 1976): 1699-1712.

23. Fouad, A. A., Vittal, V., and Taekyoo Oh. "Critical Energy for Direct Transient Stability Assessment of a Multimachine Power System." IEEE Trans., PAS-103 (Aug 1984): 2199-2206.

24. Fouad, A. A. and Vittal, V. "Power System Response to a Large Disturbance: Energy Associated with System Separation." Proceedings of 1983 PICA Conference, 1983: 116-122.

25. IEEE Committee Report. "Application of Direct Methods to Transient Stability Analysis of Power Systems." A Paper by The Working Group of The Power System Engineering Committee, PES. IEEE Trans., PAS-103 (1984): 1628-1636.

26. Fouad, A. A. "Applications of Transient Energy Function Methods to Practical Power System Problems." Presented at the Symposium on Rapid Analysis of Transient Stability, IEEE Winter Meeting, February 1986.
(Symposium Proceedings will appear in a special IEEE Publication).

27. Fouad, A. A., Ghafurian, A., Nodehi, K., and Mansour, Y. "Calculation of Generation-Shedding Requirements of B.C. Hydro System Using Transient Energy function." IEEE Trans., PWRS-1, No. 2 (1986): 17-24.

28. El-Kady, M. A., Tang, C. K., Carvalho, V. F., Fouad, A. A., and Vittal, V. "Dynamic Security Assessment Utilizing the Transient Energy Function Method." Proceedings of 1985 PICA Conference, San Francisco, CA, May 1985: 132-139.

29. Fouad, A. A., Vittal, V., Oh, T., and Raine, J. G. "Investigation of Loss of Generation Disturbances in Florida Power & Light Co. Network by the Transient Energy Function Method." IEEE Trans., PWRS-1, No.3 (1986): 60-66.

30. Fouad, A. A., Kruempel, K. C., Vittal, V., Ghafurian, A., Nodehi, K., and Mitche, J. V. "Transient Stability Program Output Analysis." IEEE Trans., PWRS-1, No.1 (1986): 2-9.

31. Fouad, A. A., Vittal, V., Rajagopal, S., Carvalho, M. A., Tang, C. K., Mitche, J. V., and Pereira, M. V. "Direct Transient Stability Analysis Using Energy Functions: Application to Large Power Networks." Paper No.86 WM066-5 Presented at the IEEE-PES Meeting, New York, NY, Feb.1986.

32. Kimbark, E. W. Power System Stability. Vol. II. New York: John Wiley & Sons, Inc., 1950.

33. Elmore, W. A., "The Fundamentals of Out-of-Step Relaying." Westinghouse Electric Corporation Relay-Instrument Division, RPL-79-1A, May 1984.

34. Westinghouse Electric Corporation Relay-Instrument Division, Applied Protective Relaying. Westinghouse Electric Corp., Coral Springs, Florida, 1982

35. Vittal, V., Oh, T., and Fouad, A. A. "Correlation of the Transient Energy Margin to the Out-of-Step Relay Operation." Proceedings of the 1985 Midwest Power Symposium, Oct., 1985: II-B-1-II-B-8.

36. Rusche, P. A., hackett, D. L., Podmore, R. L., Rhodes, R. H., and Sherke, J. E. "User's Guide to Producing Coherency-Based Equivalents for Transient Stability Studies." EPRI Report EL-2778-CCM, Dec., 1982.

37. Anderson, P. M. and Fouad, A. A. Power System Control and Stability. Ames, Iowa: Iowa State University Press, 1977.

38. Uemura, K., Matsuki, J., Yamada, I., and Tsuji, T. "Approximation of an Energy Function in Transient Stability Analysis of Power Systems." Electrical Engineering in Japan, 92, No.4 (1972): 96-100.

39. Taylor, C. W., Haner, J. M., Hill, L. A., Mittelstadt, W. A., and Cresap, R. L. "A New Out-of-Step Relay With Rate of Change of Apparent Resistance Augmentation." IEEE Trans., PAS-102 (March 1983): 631-639.

40. Haner, J. M., Lauglin, T. D., and Taylor, C. W. "Experience With the R-Rdot Out-of-Step Relay." IEEE Trans., PWRD-1 (April 1986): 35-39.

41. Roemish, W. R. and Wall, E. T. "A New Synchronous Generator Out-of-Step Relay SchemePARTS I and II." IEEE Trans., PAS-104 (March 1985): 563-582.

42. Ohura, Y., Matsuzawa, K., Ohtsuka, H., Nagai, N., Gouda, T., Oshida, H., Takeda, S., and Nishida, S. "Development of a Generator Tripping System for Transient Stability Augmentation Based on the Energy Function Method." IEEE Trans., PWRD-1 (July 1986): 68-77.

43. Johnson, L. W. and Riess, R. D. Numerical Analysis. New York: Addison-Wesley Publishing Company, 1982.

44. Dym, H. and McKean, H. P. Fourier Series and Integral New York: Academic Press, 1972.

45. Powers, D. L. Boundary Value Problems New York: Academic Press, 1972.

46. Voxman, W. L. and Goetschel, R. H. Advanced Calculus: An introduction to Modern Analysis New York: Marcel Dekker INC., 1981.

47. Podmore, R. and Germond, A. "Development of Dynamic Equivalents for Transient Stability Studies." Electric Power Research Institute Report EL-456, May 1977.

48. Kundur, P. "Evaluation of Methods for Studying Power System Stability." Proceedings of the International Symposium on Power System Stability, Ames, Iowa: Iowa State University Press, 1985: 29-36

ACKNOWLEDGEMENTS

I would like to express my deepest gratitude to my major professors Dr. A. A. Fouad and Dr. V. Vittal for their advice, encouragement, and invaluable guidance throughout this research. Their encouragement and guidance made this research possible.

Many thanks are due to my committee members, Dr. H. W. Hale, Dr. K. C. Kruempel, and Dr. R. J. Lambert for their helpful suggestions and encouragement.

I would like to thank Dr. M. W. Smiley for his helpful discussion and suggestions.

I am also indebted to the Department of Electrical Engineering and Computer Engineering and Engineering Research Institute at the Iowa State University for their financial support.

I would like to thank my wife, Hyo Sook, my son, Sang Doh, and my daughter, Sarah (MeeHae) for their constant encouragement and love throughout my graduate program.